

Final report for iBSc and MEng Group Project

**Perfusion Bioreactor for 3D Cell Culture
Investigating Adipocyte Mechanobiology**

Author name(s): Beatrice-Cristina Bezdadea, Rares-Andrei Dorcioman,
Charalambos Hadjipanayi, Emmanuel Gkigkilinis, Georgios Gryparis, Akanksha
Gupta, Goutham Sathyanarayanan, Andrew Ting

Supervisor(s): Dr Darryl Overby

Submitted in partial fulfilment of the requirements for the award of iBSc/MEng in Biomedical
Engineering from Imperial College London

March 2019

Word count: 5000

Feedback box for project markers:

WHAT I liked about the report:

WHAT could/should be improved:

Abstract

Obesity is a recognised risk factor for many cardiovascular and metabolic conditions, and with its increasing prevalence, studies are being performed to build on an existing body of research on adipocyte mechanobiology. Specifically, it is hypothesised that cyclic compression of adipocytes reduces intracellular lipid accumulation. As there are no readily available devices to investigate this theory, this project aims to develop a perfusion-compression bioreactor capable of achieving physiologically relevant strains (0%-12%) and frequencies (0.1Hz-1Hz) within a three-dimensional cell culture. A system incorporating a pump and an actuator was connected to multiple hydrogel chambers, which were computationally designed, and 3D printed. Rheological experiments were conducted to determine the optimal collagen concentration of the hydrogels. Choosing the 4mg/ml concentration, Finite Element Analysis (FEA) was used to model the behaviour of the hydrogel under compression. The results show that physiologically relevant cyclic compressions can be performed on heights less than 3.2mm, for strains of 0%, 4%, 8% and 12%. The compression system was tested separately and was found to have a 1.2% accuracy. This, together with the FEA results and the theoretical predictions about the functionality of the perfusion system anticipate that the final prototype will meet the design requirements. Therefore, this device will allow the observation of adipocyte lipid accumulation in response to cyclic compression, paving the way for further research on various cell types.

Acknowledgements

We are tremendously grateful to our supervisor, Dr Darryl Overby, whose invaluable guidance and vast expertise not only made this project possible, but also made it an absolute pleasure to work on.

We would like to thank the members of the Overby research group who have all been extremely welcoming and helpful. A massive thank you to Anabela for her never-ending patience, support, advice on hydrogels and cell culture as well as providing us with the little fatty devils. Thank you to Foivos for his help with the lyophilising, Esther for overseeing our thawing process and Kosta for helping us find our footing around the lab.

We also want to express our gratitude to Dr Joseph Sherwood for providing information and advice on the manufacturing of both perfusion and compression system components. Additionally, we would like to thank Mr Paschal Egan and Mr Niraj Kanabar for their support with the electrical design of actuator circuitry and Mrs Ji Young Yoon for her help with manufacturing of compression mechanism.

We are also thankful for the helpful insight on FEA from Dr Spyros Masouros who helped us improve our computational model of the hydrogel. Furthermore, the 3D printing could not have been done as fast without using the printers in the Biomedical Engineering Department and the Imperial College Robotics Society.

Table of Contents

1. Introduction	5
2. Design and Methods	6
2.1 <i>Design Process</i>	6
2.2 <i>The Perfusion-Compression System</i>	9
3. Results	20
3.1 <i>Design Process</i>	20
3.2 <i>The Compression-Perfusion System</i>	20
3.3 <i>Hydrogel Creation</i>	21
3.4 <i>Modelling the Hydrogel</i>	23
4. Discussion	27
5. Conclusion	30
6. References	31
7. Appendices	34

1. Introduction

Obesity, defined as “abnormal or excessive fat accumulation that presents a risk to health”[1], strongly contributes to an increased risk of heart disease, diabetes, stroke and cancer, particularly visceral fat[2]. Recently, adipocytes have been found to be mechanoresponsive, activating feedback pathways that modulate adipostasis[3] thus there is great incentive to research their mechanobiology to develop novel treatments to target and reduce visceral adipocyte hypertrophy.

Studies show that adipocyte mechanobiology[4] is dependent on the type and nature of the mechanical force applied: cyclic stretch[4] and static compression[5] have been found to inhibit pre-adipocyte differentiation, whilst static stretch promotes lipid accumulation[6]. Studies on cyclic compression could not be found in the literature. Most relevant studies were conducted in 2D cell culture, however, 3D cell culture has been shown to mimic the adipose microenvironment more accurately[7].

To house these 3D cultures, collagen hydrogels are the most widely-used and studied scaffolding, as collagen is the most abundant extracellular matrix (ECM) protein, readily available and does not require modification to support cell adhesion[4]. 3D cell cultures have the problem of non-uniform nutrient delivery, with the innermost cells receiving less due to diffusion being the limiting factor. To maintain cell viability in long term experiments, a perfusion system is needed.

Therefore, the project aims to create a perfusion bioreactor capable of providing mechanical stimulation to a 3D cell culture, to investigate the effects of cyclic compression on adipocytes. The team hypothesises that this will reduce the cells’ lipid accumulation. Devices that allow such studies are not readily available on the market, but some research groups have created custom-made ones[8-12]. These designs use recirculation of media which limits the duration of the experiments performed. To overcome this limitation, there will be separation of the fresh media and the metabolic waste.

The end-product of this project must be able to:

- Allow for simultaneous testing of different strain levels, ranging from 0% to 12%[13]
- Provide cyclic compressions with frequencies between 0.1Hz to 1Hz[13]
- Supply uniform delivery of nutrients within the cell-cultured matrix

The steps leading to the successful completion of this project are:

1. To have a parallel design allowing multiple samples to be investigated simultaneously with:
 - a. Uniform and controlled flow
 - b. Controlled strain
2. To make a computational model of the collagen hydrogel under compression
3. To record strain and flow
4. To maintain cell viability
5. To measure change in lipid accumulation in response to cyclic compression
6. To ensure safety of the device

2. Design and Methods

2.1 Design Process

Initial considerations

To achieve the parallel design objective, the bioreactor consists of 16 wells with four groups of four identical setups. Each well is connected to the uniaxial perfusion-compression system and contains a collagen hydrogel seeded with adipocytes.

The initial design of one well is shown in Figure 1. The small pore size of the membrane[14] ensures that the hydrogel would not permeate through during compression. The glass frit gives rigidity to the fragile membrane[15].

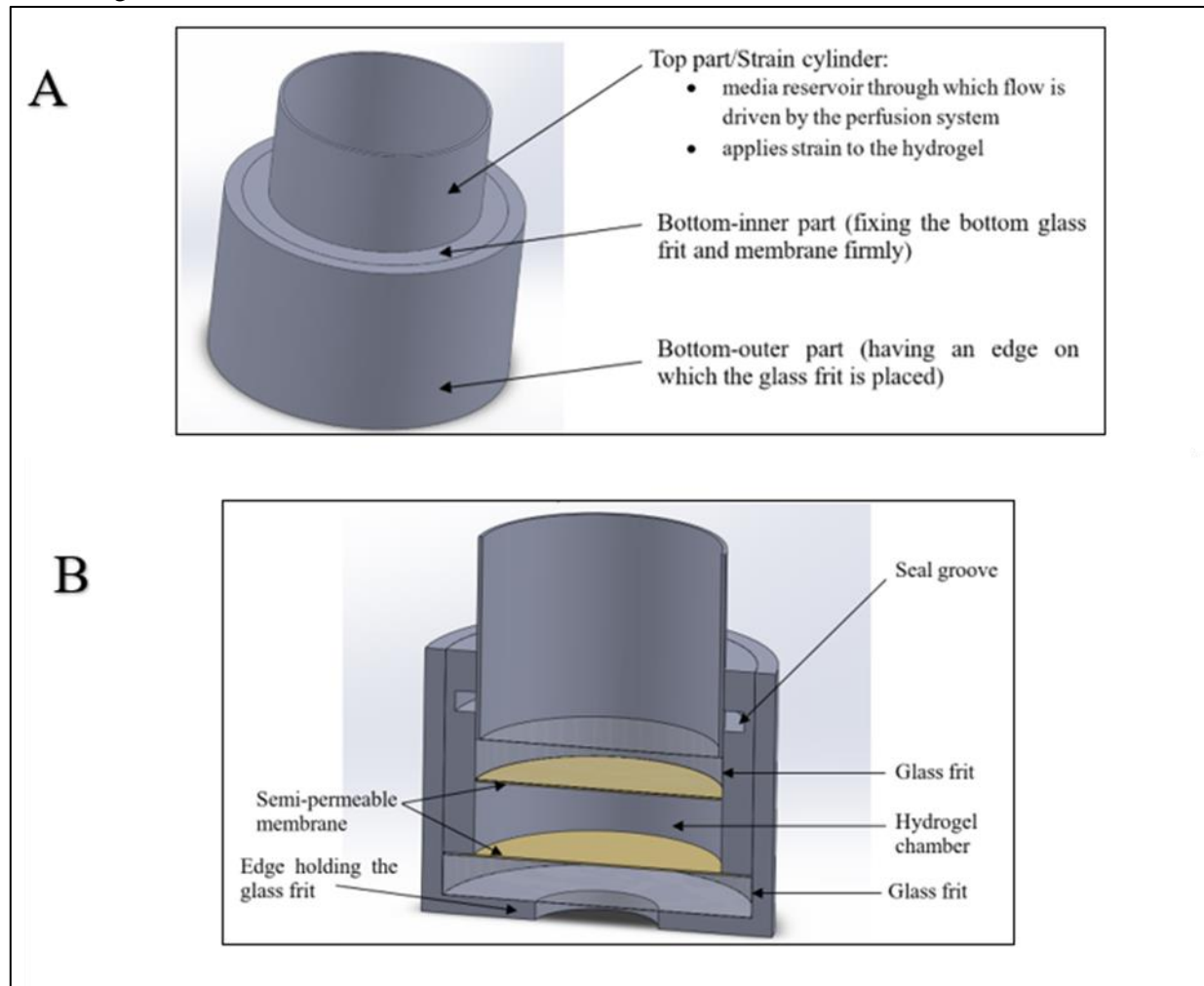


Figure 1. Initial design: **A:** components; names; functions; **B:** section view

Due to supply constraints concerning diameters of glass frits[16], the components had to be sized accordingly. Due to financial constraints, membranes already present in the lab[14] had to be used.

To ensure no leakage occurs between the components' walls, a seal was added between moving parts and adhesives were planned to be used between the static parts.

To satisfy the uniform flow requirement, the hydrogel's entire surface should be covered by the glass frit. This is because the hydraulic resistance of the frit is $1.94 \times 10^8 \text{ kg/m}^4 \text{ s}$, which is three orders of

magnitude lower than the one of the hydrogels, $4.11 \times 10^{11} \text{kg/m}^4 \text{s}$, causing the flow to spread radially inside the frit before entering the gel (Appendix A).

Manufacturing Process

The wells and compression cylinders were 3D printed, to ensure ease of changing dimensions and a quick production. The materials available were not biocompatible, but they were suitable for a proof of concept prototype. It was decided that acrylonitrile butadiene styrene (ABS) would be the best available option due to its suitability as a possible substrate for a medical-grade adhesive[17].

The 3D printers available could only print to a precision of 0.4-0.5mm, determined by attempting to print smaller thicknesses. Hence, the minimum wall thickness had to exceed these numbers. Producing a very thin wall to maximise the contact area between the glass frit and the hydrogel was consequently limited. Additionally, the 3D printers available did not possess a high level of accuracy, and to ensure dimensional compatibility, a trial and error method was used. The parts were printed with small variations in dimensions until the ideal fit between the printed parts, the glass frits and the seal was achieved. The details of each trial are shown in Appendix B. The initial design was limited because the seal did not fit inside the groove (Figure 1), which was therefore moved from the bottom-inner part to the top part. The final design is shown in Figure 2.

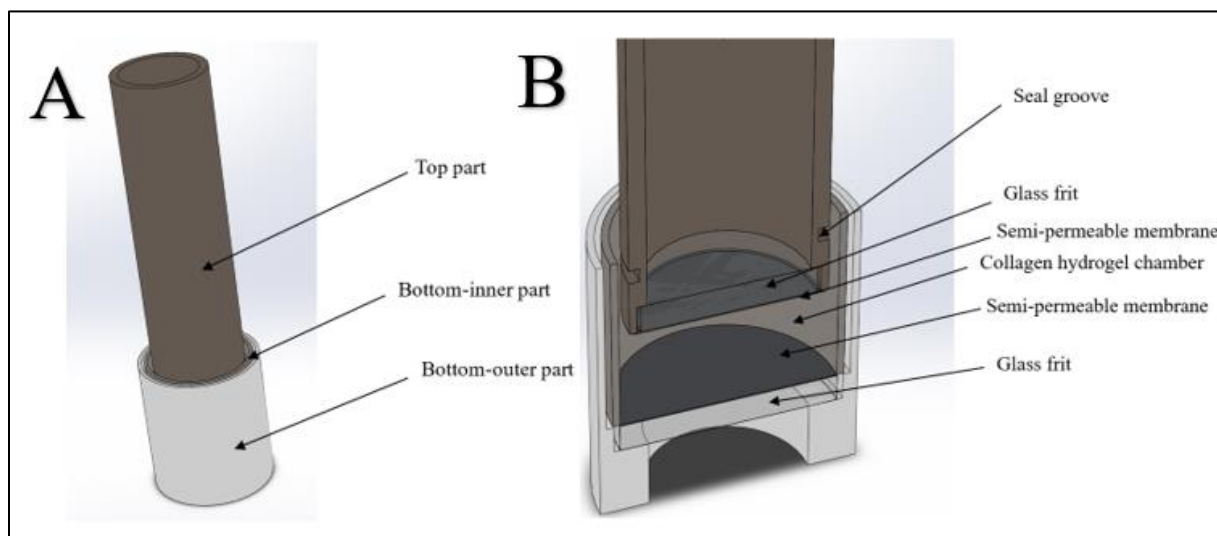


Figure 2. Final design: **A:** outside view; **B:** section view

Compression Cylinders Plate

Since the aim is to investigate physiological strain levels of 0-12%[13], the strain cylinders have specific heights, in order to exert strains of 0%, 4%, 8% and 12%. This is because the hydrogel has the same height in all wells. Figure 3 shows an aluminium plate with the connected compression cylinder plates. To ensure that the centre of gravity of the top plate is in the geometrical centre of the structure, the compression cylinders were distributed as shown in Figure 4. Due to rotational symmetry, this arrangement meant that only 2 different Computer Aided Design (CAD) files for the 3D printed plates were needed, making the design more modular.

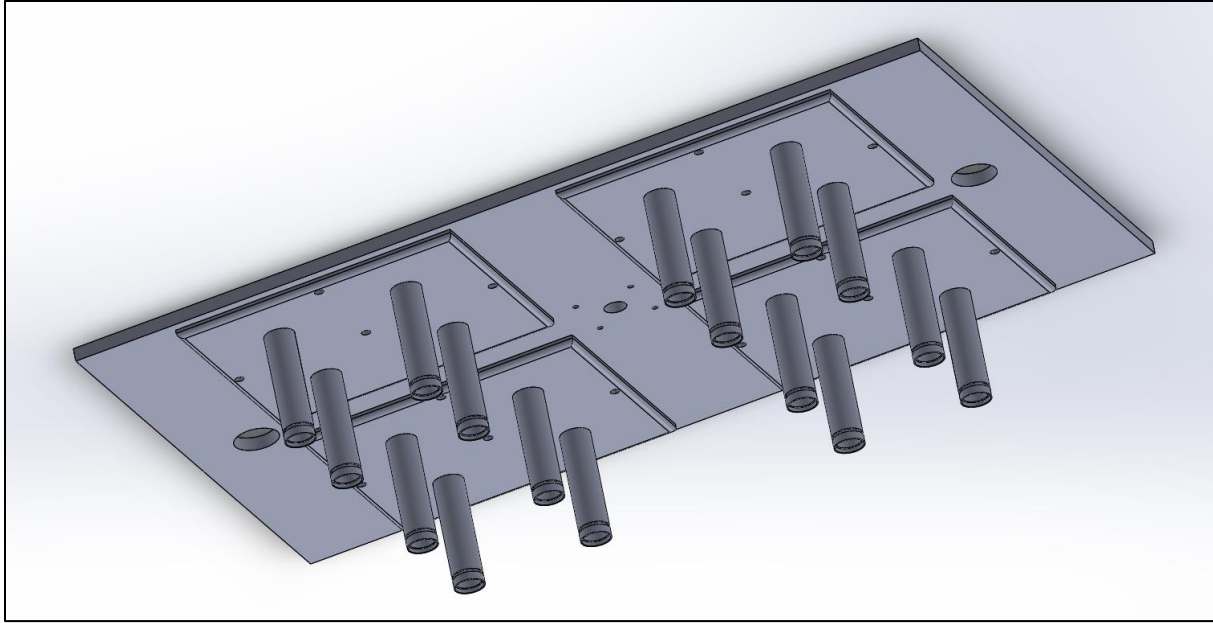


Figure 3. Compression cylinder plates

8%	4%	4%	8%
12%	0%	0%	12%
12%	0%	0%	12%
8%	4%	4%	8%

Figure 4. Strain caused by each cylinder in Figure 3 (colours show the two arrangements)

Bottom Four-Well Plate

Each compression cylinder plate corresponds to a bottom 4-well plate (Figure 5). A hydrogel seeded with cells will be placed in each well and the plate will be filled with media during the experimental setup. This is necessary step in ensuring that no air bubbles will be present within the bioreactor.

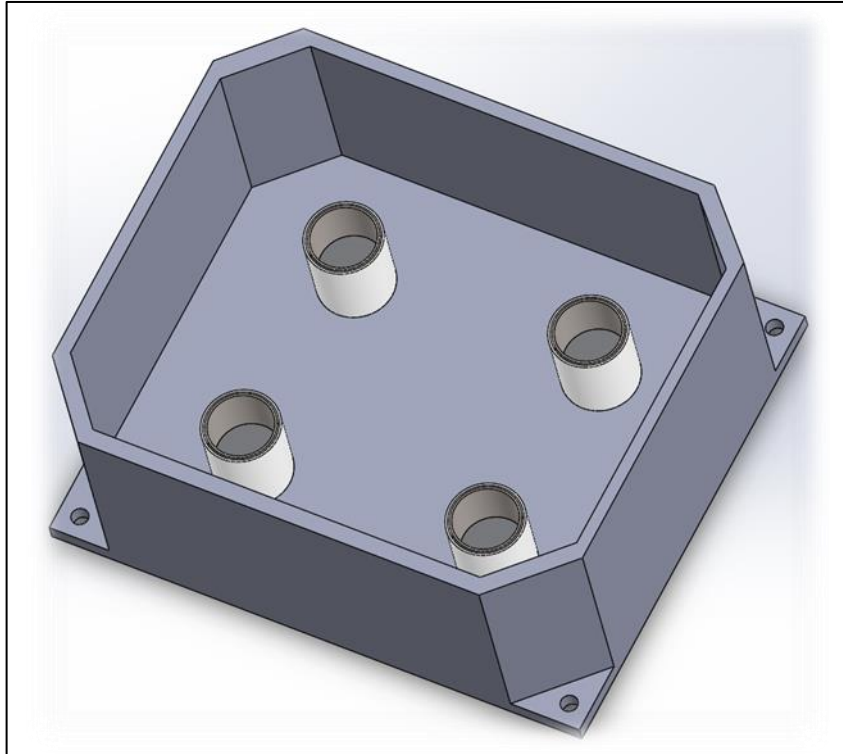


Figure 5. Bottom Four-Well Plate

2.2 The Perfusion-Compression System

Overview of instruments implemented

The complete device consists of a pump driving cell culture medium through 16 bioreactor wells that are connected to a compression system. The compression system moves cyclically producing different strain levels in each group of 4 wells at the same frequency. The whole system is controlled by a central microcontroller set up by the experimenter. The flow chart of the whole system is represented in Figure 6.

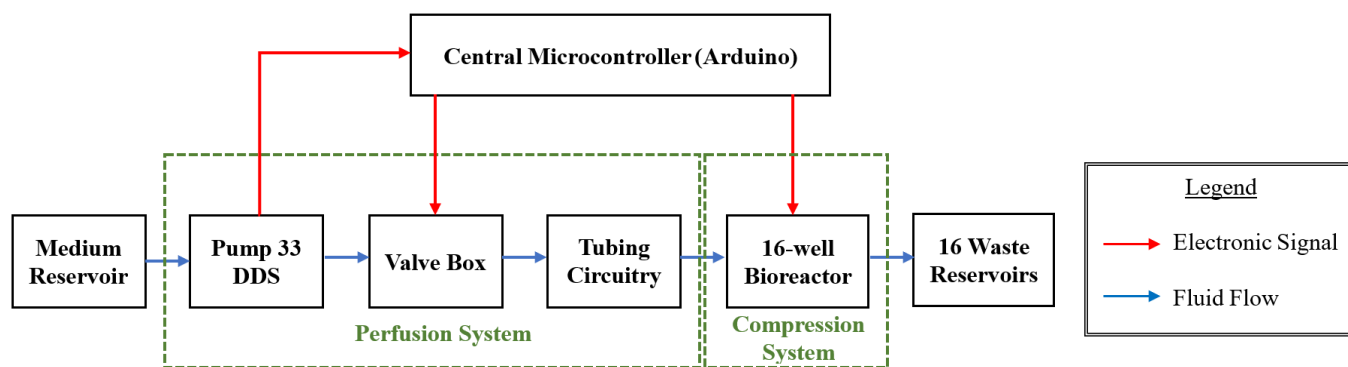


Figure 6. Flow Chart of Device

Perfusion system

The device utilises top-to-bottom perfusion to take advantage of gravity. A pump is required to supply continuous pulseless flow, in low and adjustable flow rates with high accuracy. For the application considered, a flow rate of 133nl/min is needed for each well (Appendix C). To match these requirements, a dual drive system syringe pump (Pump 33-DDS Harvard Apparatus) will be used. Its specifications are shown in Table 1.

Table 1. Pump Specifications

Specifications	Accuracy	Reproducibility	Linear Force	Min Flow Rate	Max Flow Rate
Parameter	±0.35%	±0.1%	253N	67pl/min	107ml/min

This will be operated in reciprocating mode where the two syringe channels move in opposite directions at the same rate, providing continuous fluid delivery. This requires implementing an electronically controlled valve box, consisting of two 3-way solenoid pinch valves (Cole-Parmer WZ-98302-50) each connected to a solid-state relay (Sensata/Crydom DO061A). The flow rate is chosen from controls integrated in the pump, whilst the status of each syringe (infusing/refilling) is transmitted through the pump TTL (Appendix D) output to the Arduino. The state of each valve is set by digital signals from the Arduino to the relays. A digital LOW (0V) to the relay corresponds to the valve allowing only flow from the medium reservoir, whilst a digital HIGH (5V) allows flow only towards the bioreactor. Valve control and synchronisation with the pump is achieved using the code in Appendix E and verified using LED indicators.

Figure 7 shows the perfusion system operation with syringe 1 infusing (flow towards bioreactor) and syringe 2 refilling (flow from medium reservoir).

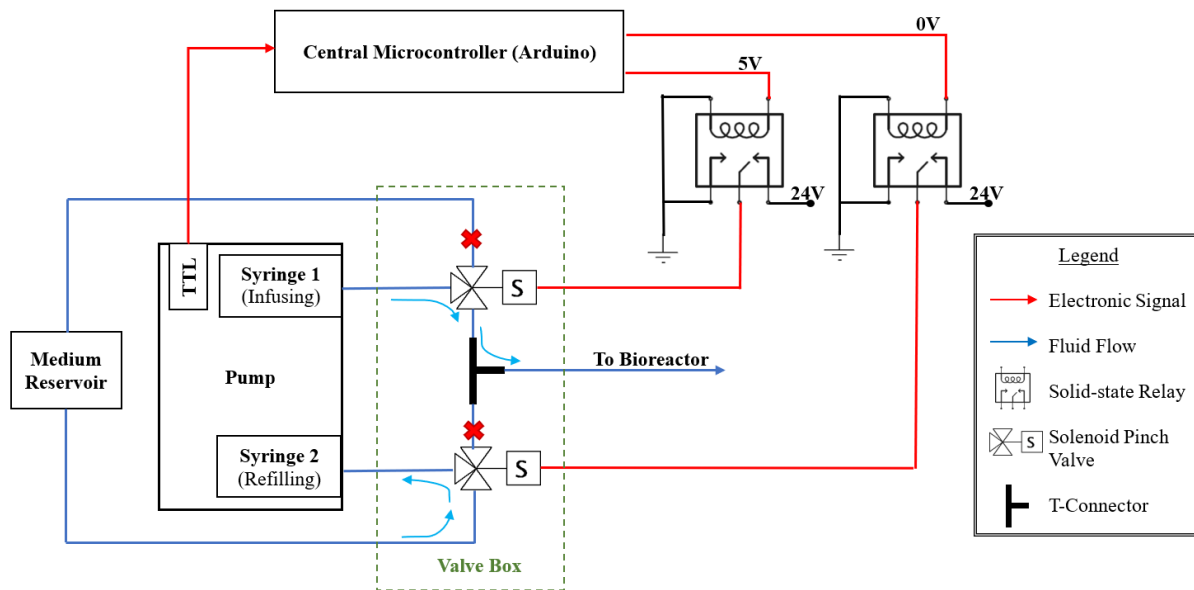


Figure 7. Perfusion System

The pump output will be split across all samples in the 16 wells, using a cascade of T-connectors (Figure 8). Biocompatible medical tubing and connectors made of polyvinyl chloride (PVC) will be used.

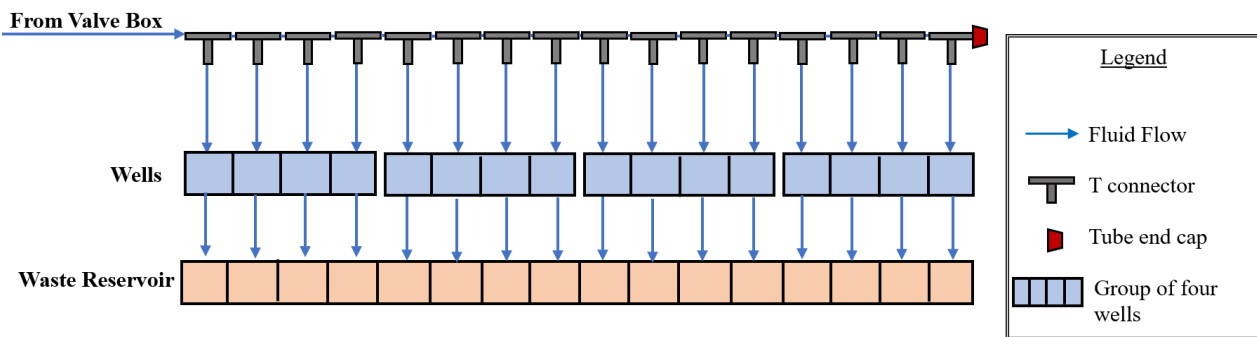


Figure 8. Tubing Circuitry

The hydraulic resistance of each hydrogel is in the order of $10^{11} \text{kg/m}^4 \text{s}$. Performing an order of magnitude calculation on the resistance of each of the 16 branches of the tubing circuitry results in a value of order $10^9 \text{kg/m}^4 \text{s}$. This suggests that the total resistance of each branch is dominated by the hydrogel resistance. Therefore, the flow will be split evenly across all wells (Appendix F).

Each well is connected to a separate waste reservoir using a stopcock and a one-way valve, which functions to ensure air does not enter the system and no backflow occurs during the upward motion of the actuator. The flow rate through each sample can be deduced from the volume of media accumulated in each separate reservoir over a given amount of time. Additionally, having separate waste reservoirs allows for analysis of metabolites from each individual sample.

During the initial filling phase, all wells are fully submerged in culture media and their outlets are blocked. The strain cylinders are placed a small distance below the culture media surface.

The pump is then activated, filling the strain cylinders with media. Once they are filled, the strain cylinders are attached to the hydrogel chambers, followed by opening of the outlet channels. This ensures the absence of air in the bioreactor.

Compression system

Physiological compressive frequencies range from 0.1Hz to 1Hz[13]. The required strains on the hydrogel are between 0% and 12%[13]. Through computational analysis and experimentation, it was determined that the maximum compressive force required per well is below 9N and is dominated by friction (Appendix G) The Nanotech L35 series linear actuator (L3518S1204-T6x1) was chosen as it fits the specifications (Table 2).

Table 2. Actuator Specifications

Maximum Force (N)	Maximum Velocity (mm/s)	Resolution (mm)
240	5	0.005

Table 4 suggests that a maximum force of 15N can be applied to each hydrogel. Additionally, it can be shown that for constant velocity compressions, the actuator’s maximum velocity allows for frequencies larger than 1Hz for hydrogels of height smaller than 20mm (Appendix H). The actuator’s resolution implies that for hydrogel heights larger than 5mm the error in the strains applied is smaller than 0.1%. For hydrogels smaller than 5mm in height, an appropriate motor driver that allows microstepping will be used to improve resolution (Appendix I).

The actuator’s motion is dictated by the central microcontroller. The Nanotech SMC11 microstep is employed to convert the Arduino logic output to stepper-motor driving currents. A microstep driver provides the option to improve resolution in exchange for higher power consumption. The SMC11 can improve resolution by up to 800% by microstepping and has a 50% current reduction mode that can be used in cases of static compression to reduce heat generation. The actuator control system is shown in Figure 9 (code in Appendix J).

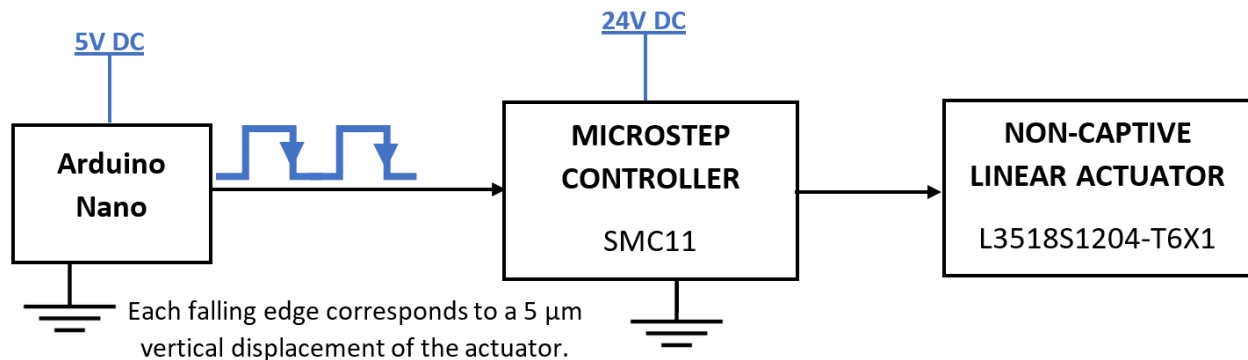


Figure 9. Compression system

To translate actuator motion into mechanical strain on the samples, a construct is designed composed of two 6mm thick aluminium plates and two 16mm diameter stainless steel rods (Figure 10).

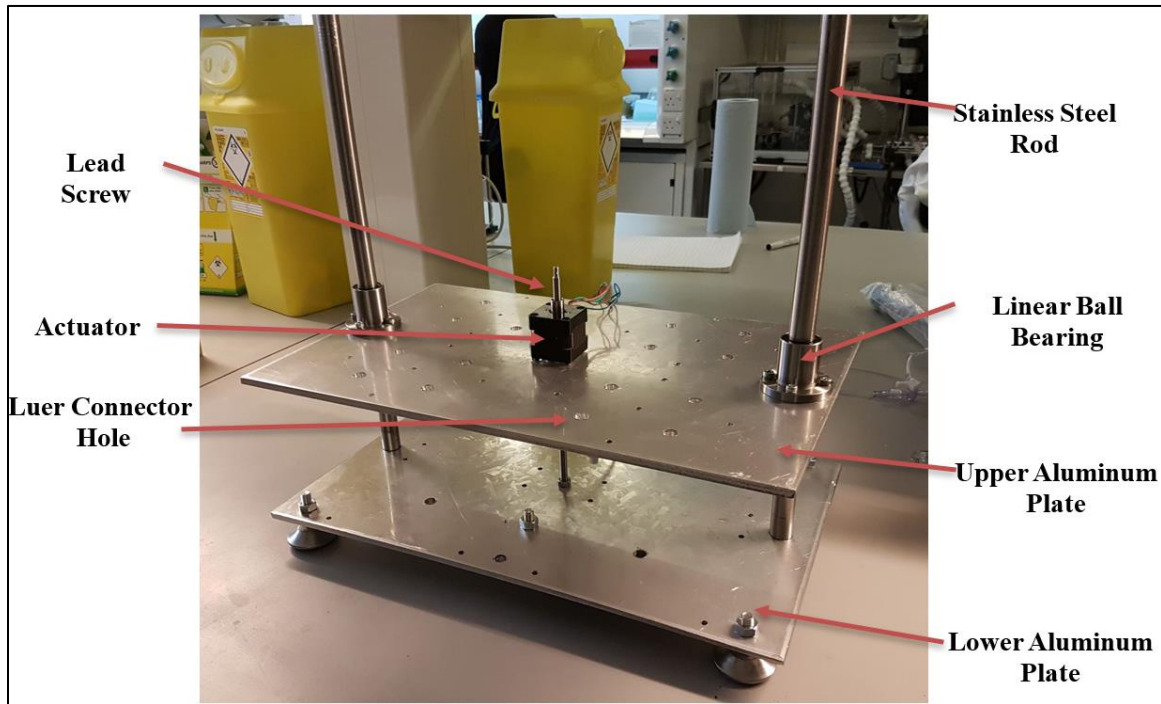


Figure 10. Manufactured compression mechanism

The actuator and strain cylinders will be attached to the upper plate with bolts (Figures 3, 10). The tubes of the perfusion system will be linked to the interior of the strain cylinders via Luer connectors. Holes were drilled in the top plate, allowing the connectors to pass through.

The actuator moves vertically on a lead screw (Nanotec SCREW-ABA-TJBA-200) connected to the lower plate that supports the weight of the upper plate and strain cylinders. The upper plate is guided by two rods attached to the base to ensure that the displacement does not deviate from the vertical axis and there is no rotational motion in the actuator. The rods are threaded at the bottom and screwed in securely. Lubricated linear ball bearings (LMEF16UU) on the upper plate are used to minimise friction whilst only allowing vertical motion.

The compression system is programmed to respond to a single pulse from the Arduino with a $5\mu\text{m}$ vertical displacement of the upper plate. This level of precision could not be examined experimentally using readily available equipment. However, the relationship between logic input and displacement was verified to $20\mu\text{m}$ accuracy by using a high precision Vernier calliper and inputting pulses using a signal generator.

An aluminium based alloy (Grade-1050) was chosen for the upper plate as it can support the mechanical stresses present without deforming, is corrosion resistant and has lower density than other metal alloys. The latter is particularly significant as it decreases the load on the actuator. The weight of the upper plate is approximately 1.7kg, corresponding to 7.1% of the actuator force capacity.

Stainless steel rods were chosen as they are resistant to corrosion and can withstand the actuator's torque with no deformation. As the rods are only attached to the base, weight is not a factor in the choice of rod material.

2.3 Hydrogels

Making the hydrogel consisted of three distinct parts: culturing the adipocytes, creating the collagen hydrogel for the adipocytes to be seeded into, and rheometry.

The first step to culturing the adipocytes was to thaw frozen precursor 3T3-L1 mouse fibroblast dated July 2018, on their 27th passage. Cell passage was performed according to standardised protocol (Appendix K) and culture media (DMEM/FBS) was changed every alternate day until there were enough cells to seed at a concentration of 50,000 cells/ml. Trypan blue's efficacy at measuring cell viability throughout the experiment was tested upon the HeLa cell line (Appendix L).

To create the collagen hydrogel, tendons were manually extracted from rat tails, which are densely Type-1-collagenous structures. They were then left in acetic acid to solubilise for 48 hours at 4°C (Figure 11) as stipulated in the protocol (Appendix M). Centrifugation and lyophilisation followed.

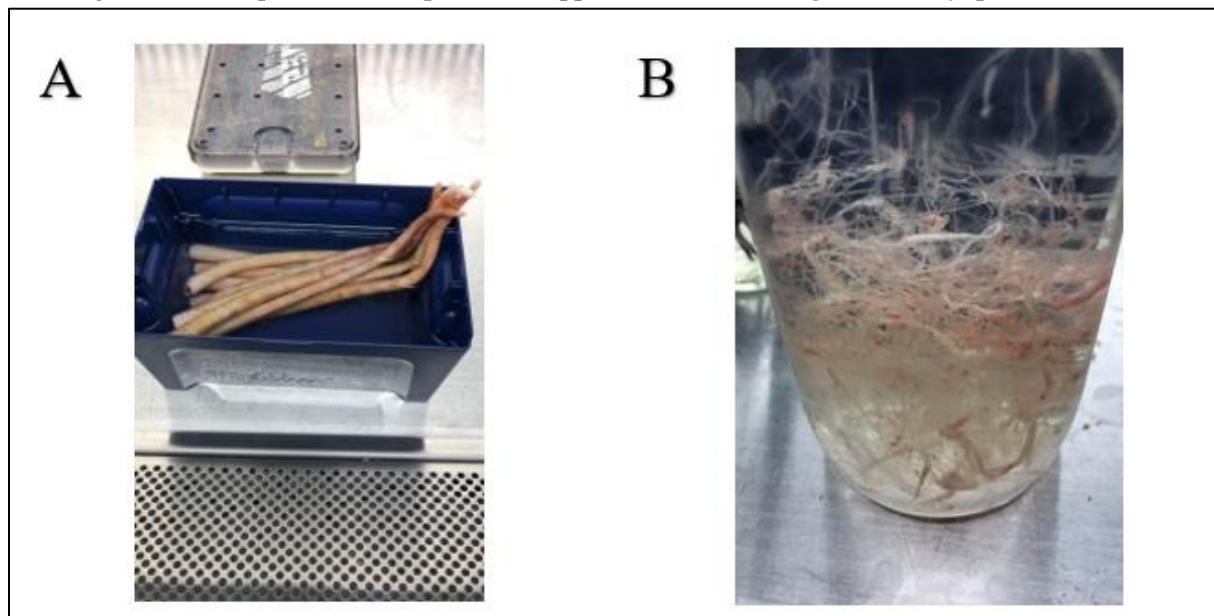


Figure 11. A: Rat tails; B: Tendons in acetic acid

Post-lyophilising, four different amounts of collagen were weighed out to create four different concentrations (1, 2, 4 and 8 mg/ml), by reconstituting in 0.1% acetic acid (Figure 12) for rheometry. To allow time for sufficient mixing, the protocol in Appendix N was followed to make the hydrogels from the resulting solution.

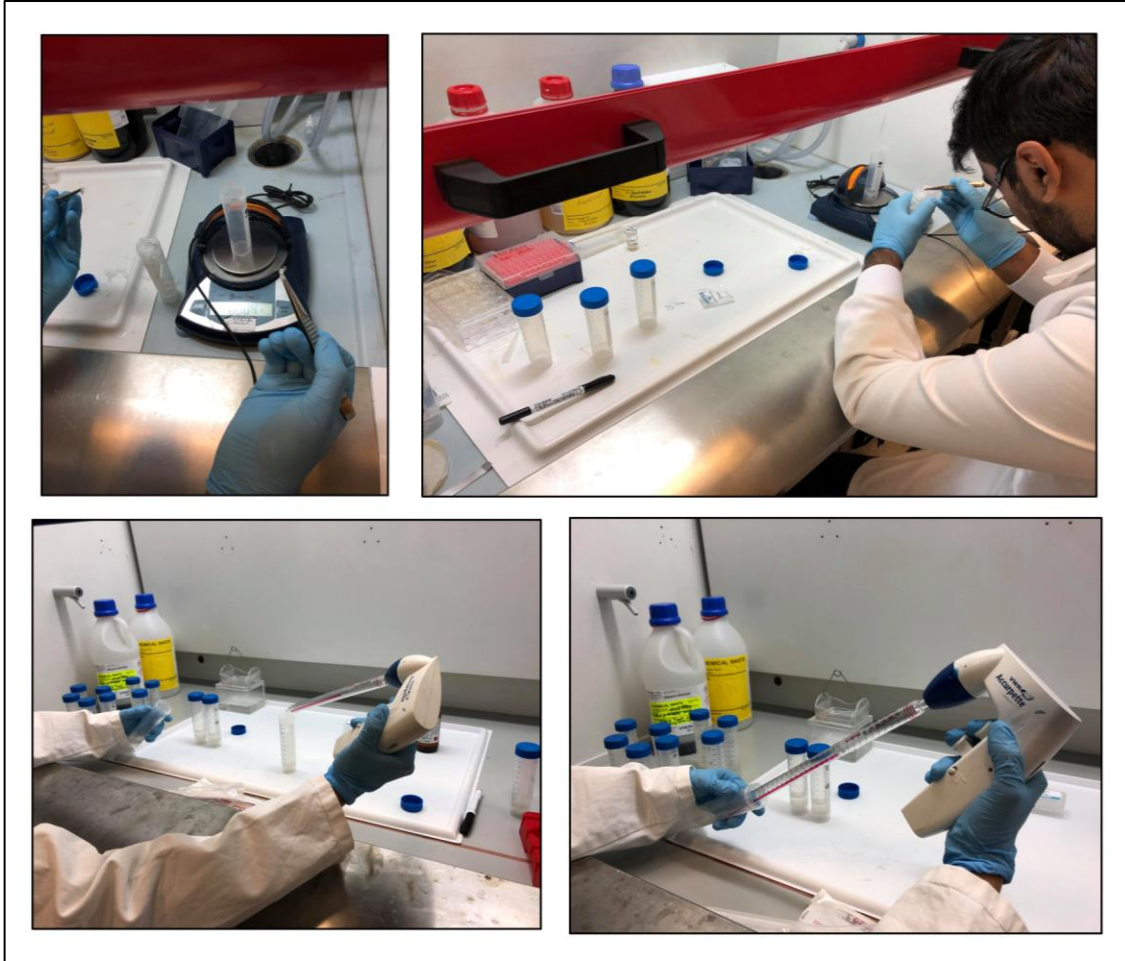


Figure 12. Reconstituting the amounts of collagen with appropriate volumes of 0.1% acetic acid

The choice of collagen concentration of hydrogel to be used is based on its viscoelastic properties. Rheological experiments were conducted, as they are sensitive to property changes between different collagen concentrations[18]. For each sample, 1ml of hydrogel was prepared as described in Appendix O. The machine used was a TA Instruments AR2000EX Rheometer. The geometry used was a 40mm diameter cone with a 2° angle. The estimated volume needed for the sample to fill the space under the cone when the tip reaches the bottom plate was 580 μ l (Figure 13). Since it was not possible to accurately estimate the centre, 700 μ l of solution was added (Figure 14(a)) and the excess was removed. The final setup is shown in Figure 14(b). The hydrogel was added with the bottom plate at 5°C to avoid polymerisation occurring before the cone plate came in contact. The sample was left for 25 minutes at 37°C for the collagen fibres to form cross-links. The experiment was performed with the setup shown in Appendix P.

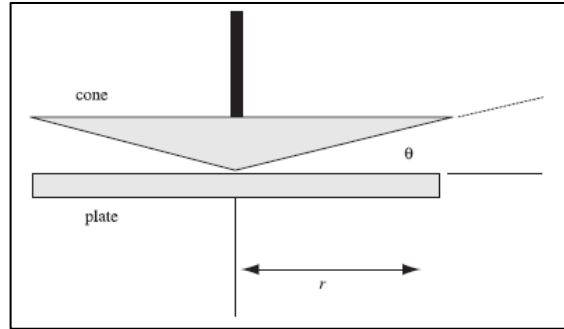


Figure 13. Cone-plate geometry schematic

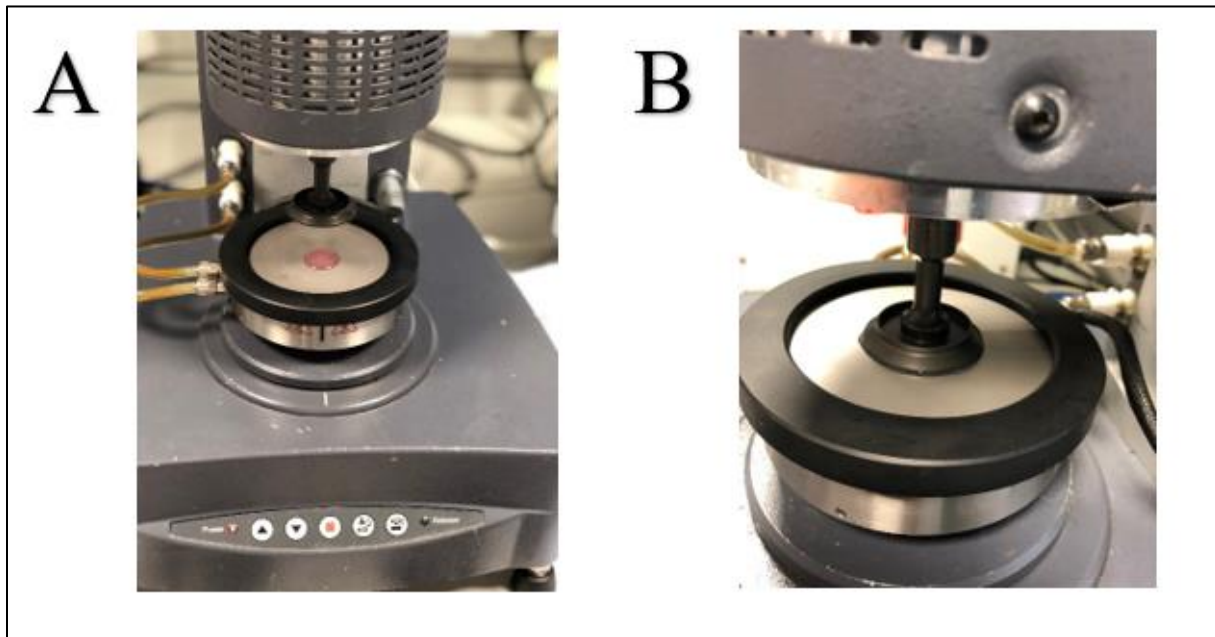


Figure 14. Rheometry setup: **A:** Loaded hydrogel; **B:** Hydrogel at zero geometry gap

2.4 Computational Model of the Hydrogel Compression

A computational hydrogel model experiencing compression was used to determine if the hydrogel could undergo cyclic compressions. This depends on how fast the hydrogel relaxes back to 5% of the strain applied, after the stress is removed. To undergo cyclic compressions at physiological levels (0.1-1Hz)[13], the maximum relaxation time must be 10s, corresponding to a 0.1Hz compressing frequency[18].

The simulation was performed using FEBio[19]. As Finite Element Analysis (FEA) requires a validation method, a theoretical confined compression of a poroelastic material[20] had to be simulated. The geometry is shown in Figure 15. It is considered that at time $t = 0^+$ the porous platen moves down a distance u_0 infinitely quick such that a small compressive stress is applied. Using MATLAB (Appendix Q) the displacement distribution was calculated at increasing times until a steady state was reached.

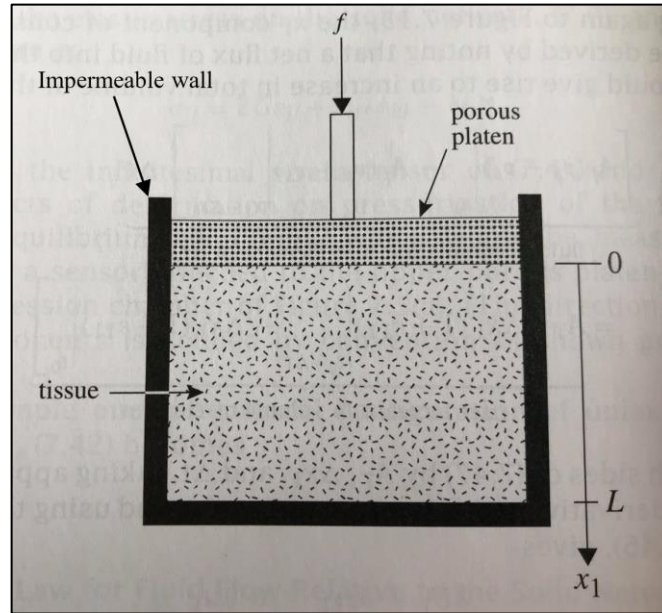


Figure 15. Validation problem geometry[20]

2.5 Theoretical Problem Simulation and Representative Hydrogel Modelling

Table 3 shows the parameters used for two simulations: one with a porous top and one with a porous top and bottom. The dimensions correspond to 0.4ml of hydrogel with 4mg/ml collagen concentration. For the validation model, the case with a porous top and the load corresponding to 10% strain were used. The indices of the surfaces are shown in Figure 16. There was a single analysis step: compressing surface 6 to observe the steady state displacement profile of the hydrogel.

Table 3. Hydrogel simulation parameters

Body–Cylinder	<ul style="list-style-type: none"> • Height: 0.002294m (Section 3) • Radius: 0.00745m (Section 3)
Material–Biphasic: Isotropic elastic Constant permeability	<ul style="list-style-type: none"> • Solid volume fraction: 0.04[21] • Young’s modulus: 565.7251Pa • Poisson’s ratio: 0.475[22] • Permeability: $0.8 \times 10^{-10} \text{m}^4/\text{Ns}$[22]
Boundary conditions	<ul style="list-style-type: none"> • Fixed X,Y displacement of surfaces 2,3,4,5 • Fixed X,Y,Z displacement of surface 1 • Relative fluid pressure=0 for: <ul style="list-style-type: none"> Porous top: on surface 6. Porous top and bottom: on surfaces 1,6.

Loads	<ul style="list-style-type: none"> • Surface traction on surface 6: <ul style="list-style-type: none"> ○ -152Pa (4% strain) ○ -285Pa (8% strain) ○ -344Pa (10% strain) ○ -400Pa (12% strain) • Fluid volumetric flow rate=0 for: <p style="margin-left: 20px;">Porous top: on surfaces 1,2,3,4,5.</p> <p style="margin-left: 20px;">Porous top and bottom: on surfaces 2,3,4,5</p>
-------	--

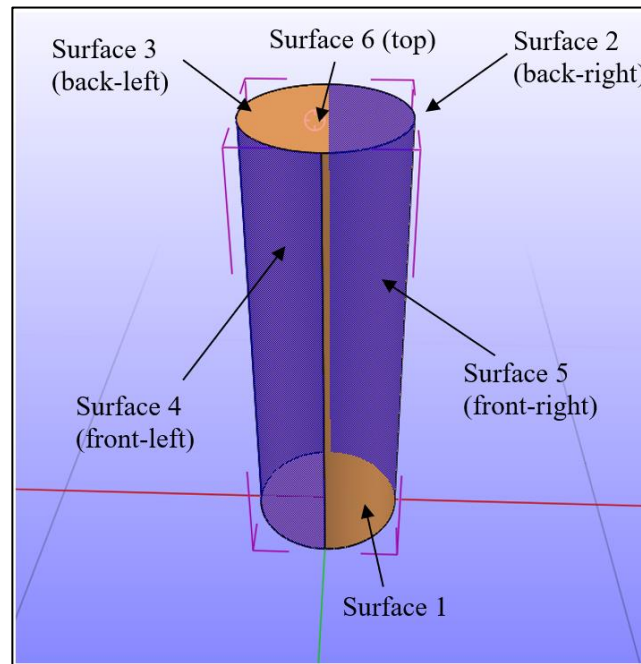


Figure 16. Surface indices of the body

Hydrogels are similar in composition with cartilaginous tissues[23], which are characterised using biphasic theory[24]. Therefore, a biphasic material was chosen. During rheometry, the hydrogel’s storage modulus, G' , was found to be much higher than its loss modulus, G'' , so the solid part of the material was modelled as linear elastic.

Young’s modulus (E) was obtained using equations 1 and 2:

$$|G^*| = \sqrt{G'^2 + G''^2} \tag{1}$$

$$E = 2 \cdot |G^*| \cdot (1 + \nu) \quad \text{where } \nu = \text{Poisson's ratio} \tag{2}$$

Strains of 4%, 8% and 12% were investigated. The strains were implicitly obtained by applying appropriate compressive stresses (Appendix R), as prescribing the strains directly results in an infinite force and cannot be analysed with FEBio.

The mesh is finer at porous boundaries to better capture the rapid fluid pressure variation when passing from inside the tissue to the outside. The mesh for each model was found (Appendix S) by performing convergence tests until the relaxation time remained constant for an increasing number of nodes.

A representative hydrogel model was developed from experimental data. Simulations were conducted for various volumes, using the parameters in Table 3 (porous top and bottom case), with the height being the only change. A two-step analysis was performed: compressing the hydrogel to the desired strain and releasing the stress at time $t = 2s$, allowing it to relax.

3. Results

3.1 Design Process

The final dimensions of the well design are shown in Figure 17.

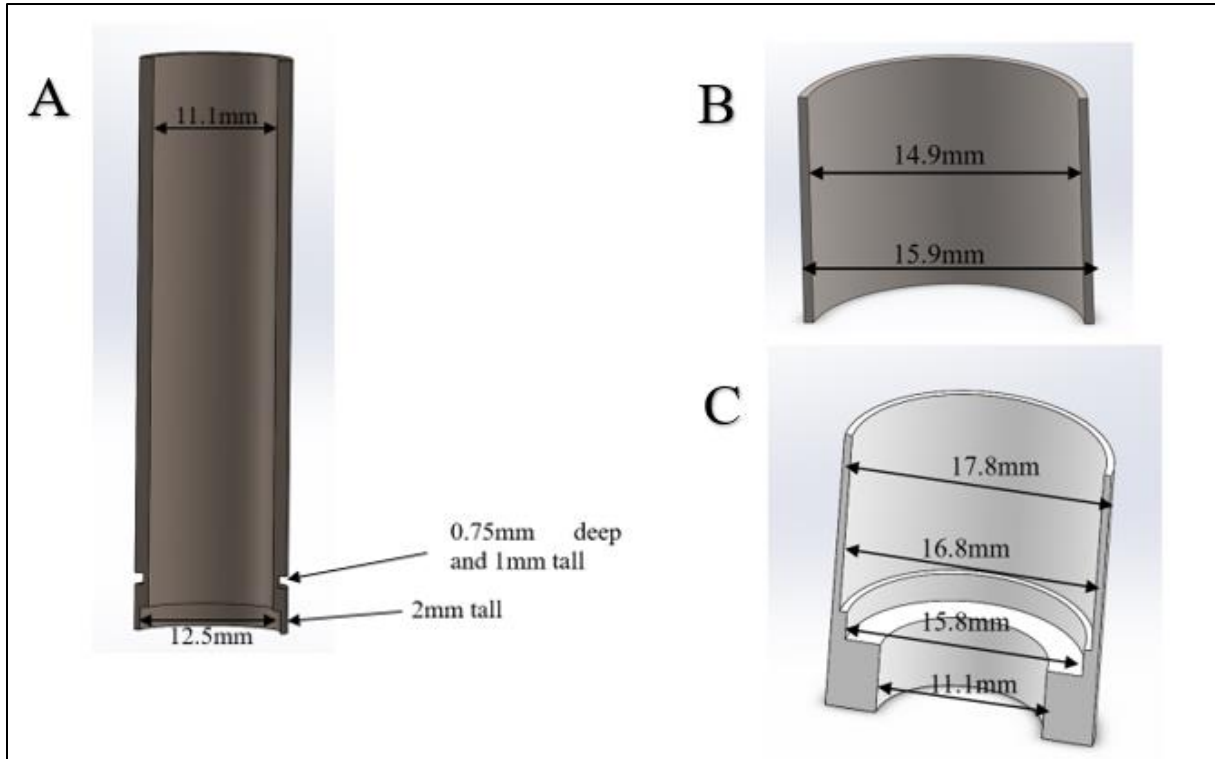


Figure 17. Well component dimensions: A: top part; B: bottom-inner part; C: bottom-outer part

3.2 The Compression-Perfusion System

Figure 18 depicts the relation between number of pulses and displacement as measured experimentally. All values obtained are within $40\mu\text{m}$ and the slope is within 1.2% of the theoretical prediction (experimental data in Appendix T).

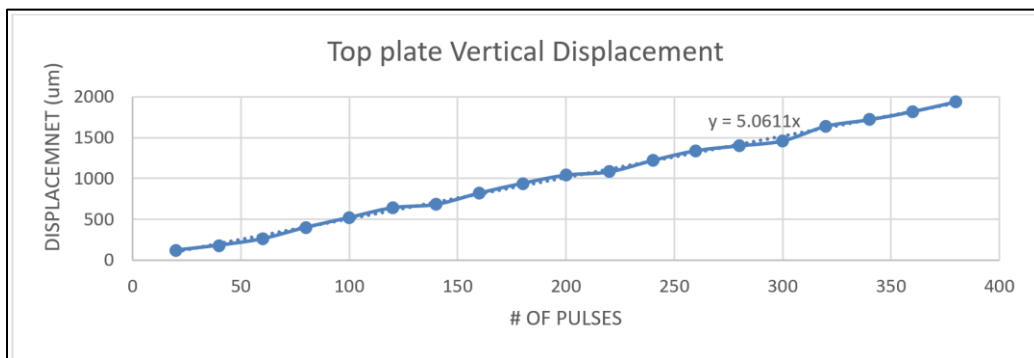


Figure 18. Digital input vs. compression plate displacement

3.3 Hydrogel Creation

Cell Culture

Due to unforeseen circumstances, the number of 27th passage 3T3-L1 cells that survived the thawing process was insufficient to begin the seeding and differentiation processes.

HeLa cells were cultured as an interim to provide a positive control for the efficacy of trypan Blue (Figure 19).

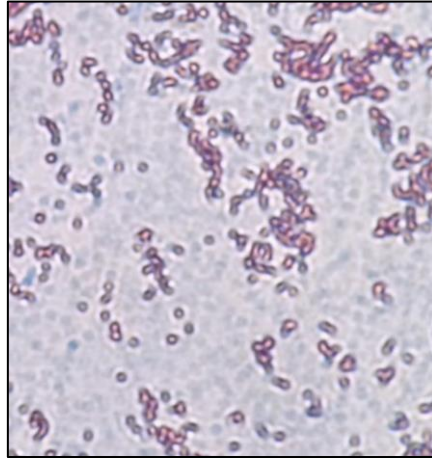


Figure 19. *Trypan blue stained HeLa cells*

As described in Appendix C, if the bioreactor is loaded with 50,000 cells/ml, the flow needed to perfuse the construct is 20 μ l/h.

Rheometry

The rheological experiments results are shown in Figure 20, and summarised in Table 4. These were used to calculate the mechanical characteristic of the hydrogel.

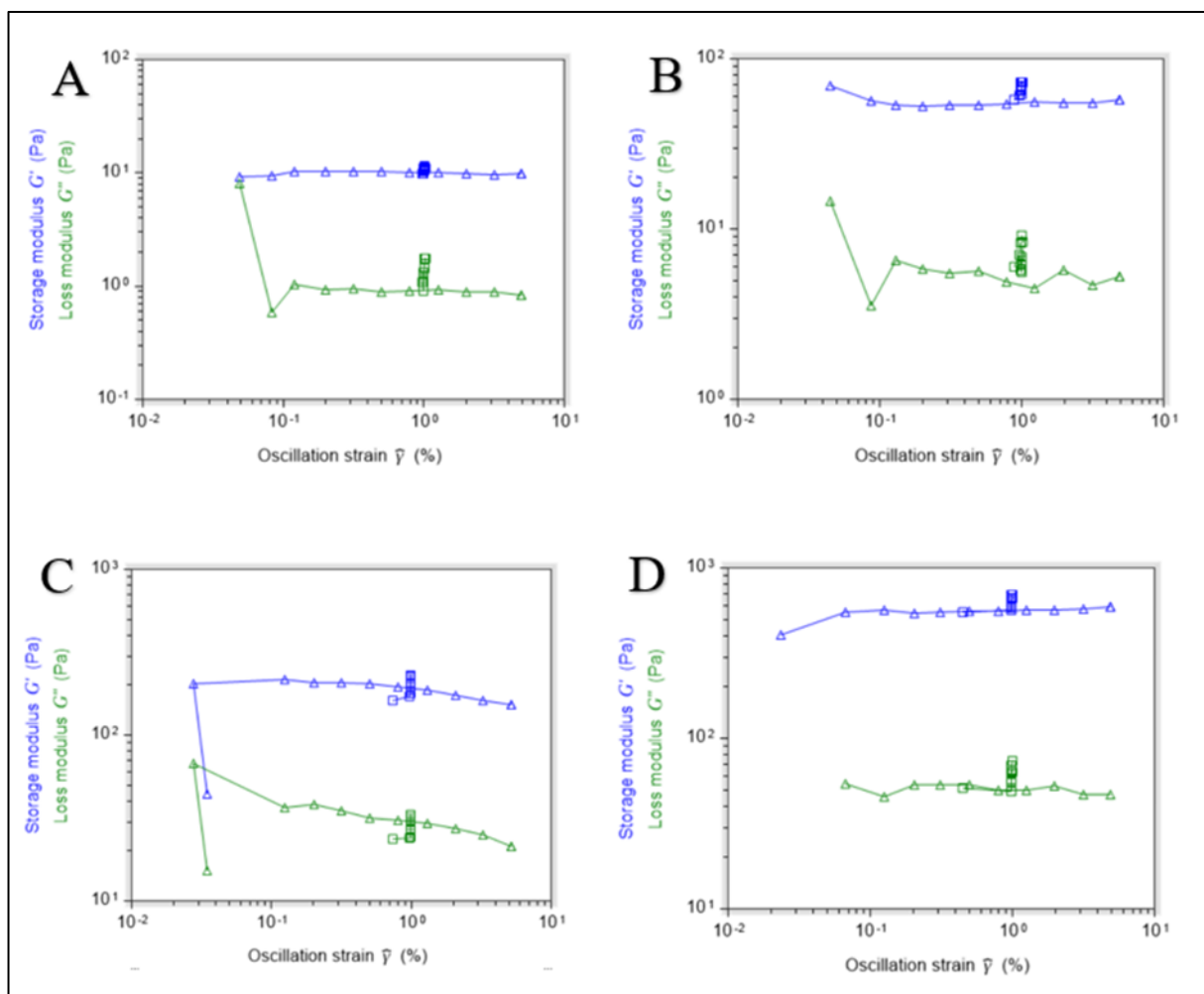


Figure 20. Rheological data different hydrogel concentrations:
 A) 1mg/ml, B) 2mg/ml, C) 4mg/ml, D) 8mg/ml

Table 4- Rheological data summary (mean \pm standard deviation)

	Concentration (mg/ml)			
	1	2	4	8
G' (Pa)	9.918 ± 0.371	56.076 ± 4.546	190.805 ± 48.547	548.230 ± 50.356
G'' (Pa)	1.540 ± 2.170	6.261 ± 3.553	34.272 ± 12.723	50.541 ± 3.440

3.4 Modelling the Hydrogel

Computational Model Validation

The displacement profile evolution in time obtained with the MATLAB model described in Appendix Q (Figure 21(a)) resembles the theoretical result (Figure 21(b))[20].

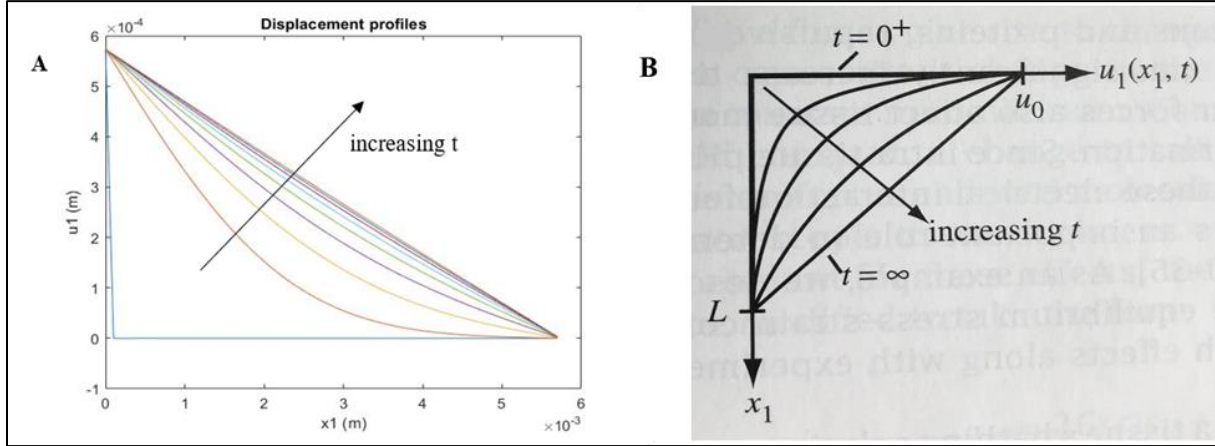


Figure 21. Displacement profiles from: **A:** MATLAB simulation **B:** Textbook[20]

The time constant is $\tau_1 = 10.3226$, and at a time $t = 3 \cdot \tau_1$, the profile is 99.88% linear (linear regression $R^2 = 0.9988$) as shown in Figure 21. Hence, it makes a good approximation of the steady state reached at $t = \infty$.

The FEBio simulation outcome matched the theoretical results plotted using MATLAB, which confirms the reliability the computational methods used. Thus, subsequent simulations can be performed using the representative hydrogel model.

The investigated nodes and corresponding displacement profiles are shown in Figure 22.

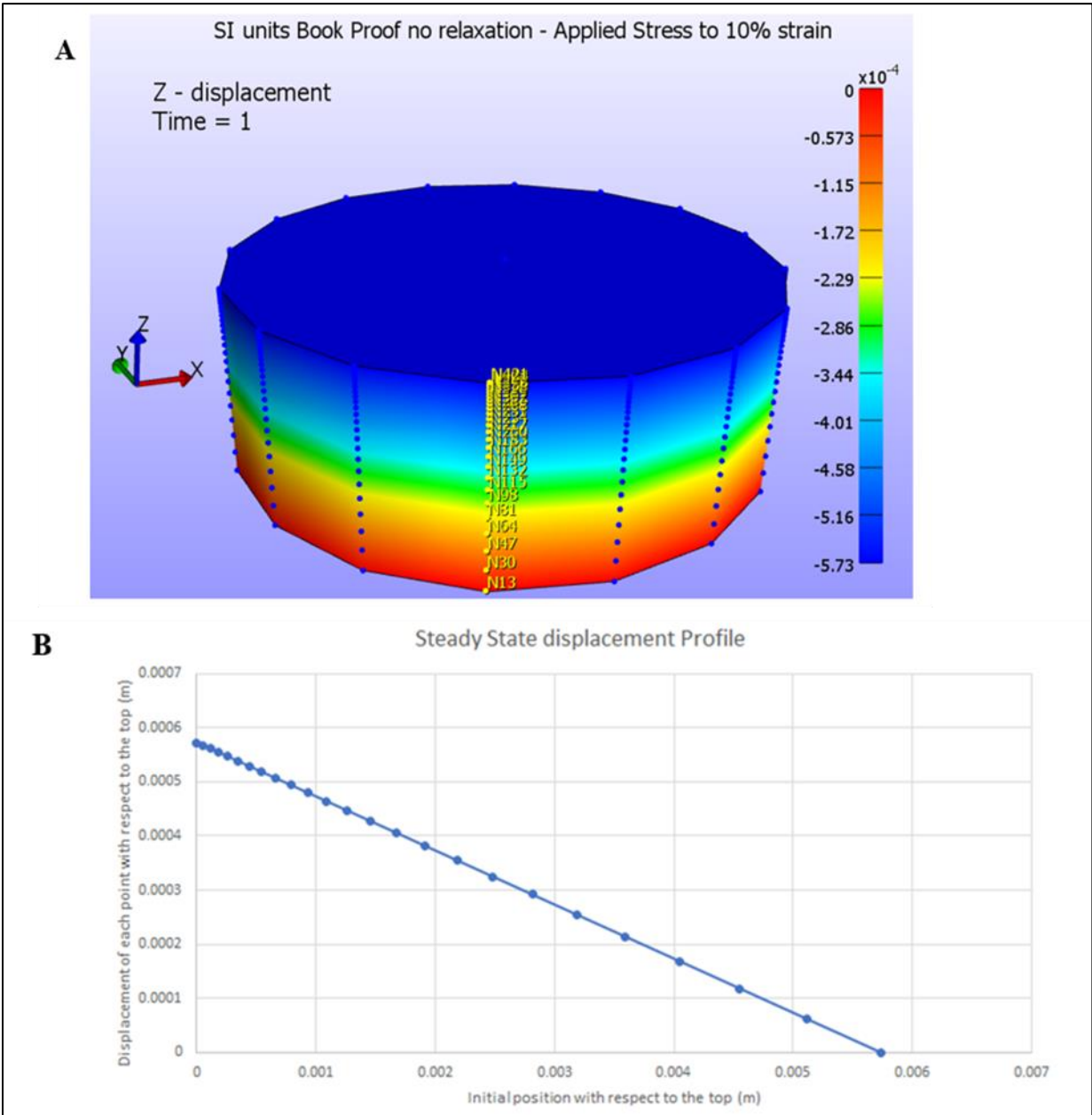


Figure 22. A: Steady state displacement of specific nodes; B: Displacement profile of the nodes

Representative Hydrogel Model

The results are shown in Figure 23. The values on which this is based are tabled in Appendix U.

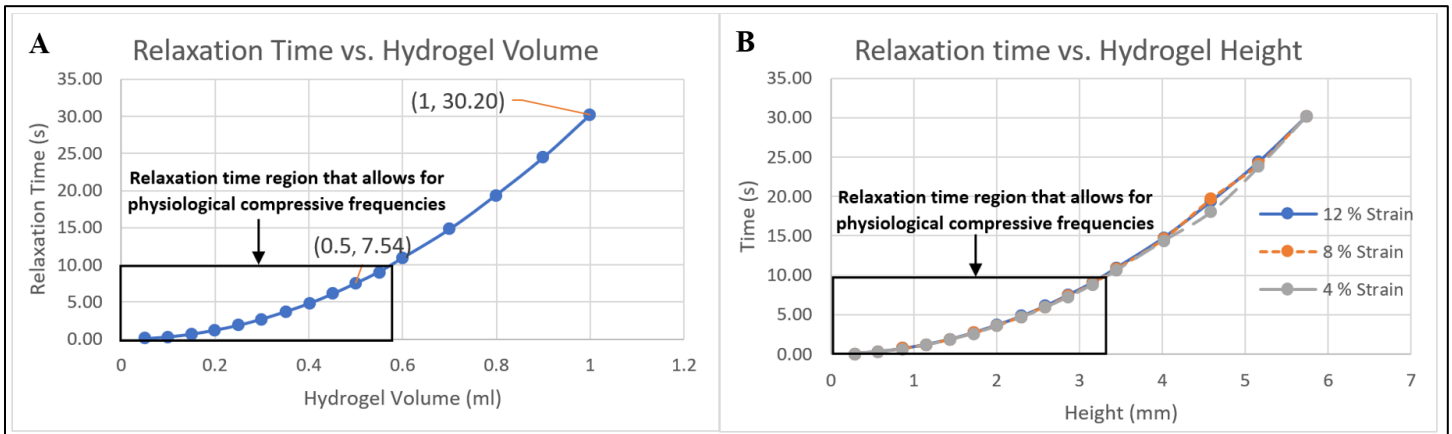


Figure 23. A: Relaxation time vs. volume **B:** Relaxation time vs. height

Figure 24 shows the case for a 0.4ml hydrogel volume and 8% strain. The time to reach 5% of the initial strain applied after the stress is removed (at $t = 2s$) is 4.75s. Examples for other strains are shown in Appendix V. Figure 25 shows the displacement profile of the top face.

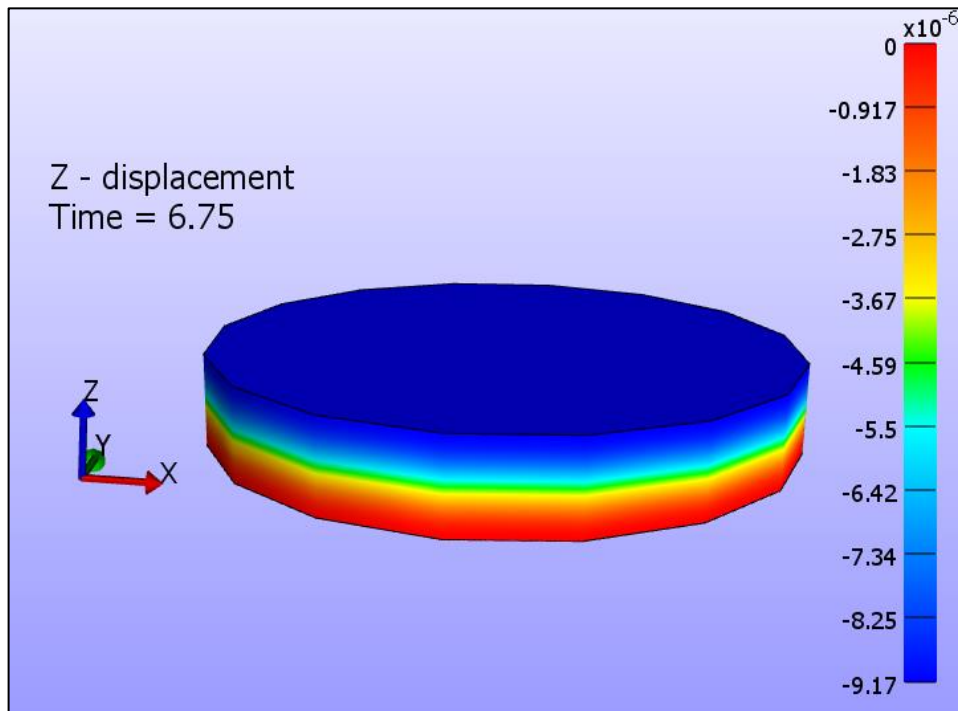


Figure 24. Displacement profile for 8% initial strain (relaxation time = 4.75s)

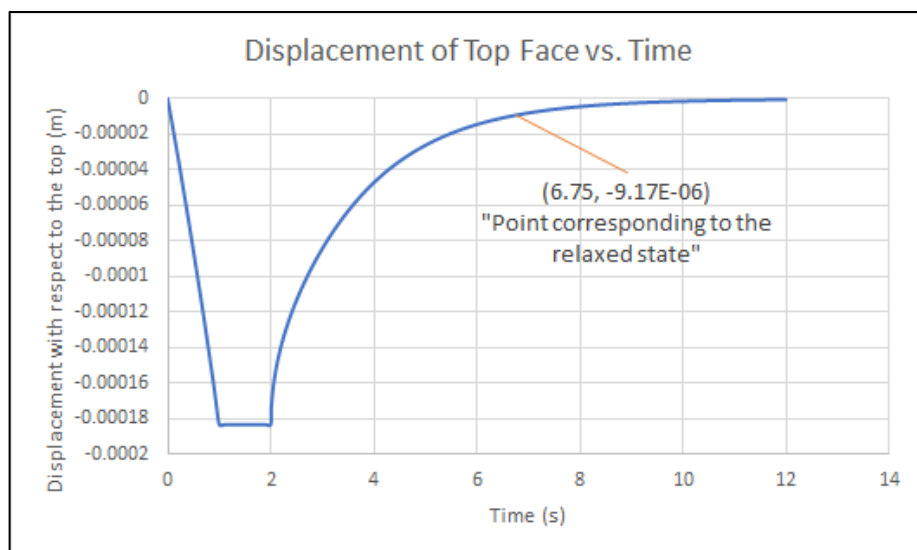


Figure 25. Displacement of top face vs. time for 0.4ml of hydrogel and 8% strain

4. Discussion

The proposed device was evaluated using computational analysis and shown to be compatible with the design requirements. As shown in the Results section, the theoretical displacement profiles, MATLAB simulation, and FEBio validation model are consistent (Figures 21-22). Hence, the FEA results obtained throughout this project are reliable.

The simulations indicate that the time taken for the hydrogel to relax to 5% of its initial strain is within physiological conditions (maximum 10s) for hydrogel volumes smaller than 0.55ml (Figure 23). This figure also illustrates that the relaxation time scales with approximately the square of the volume. For volumes lower than 0.18ml, the relaxation time is less than 1s. Therefore, the full range of physiological frequencies (0.1-1Hz)[13] could be investigated. A volume of 0.4ml was chosen as a balance between experimental errors and implementable frequencies.

To investigate the compressive effect of the perfusion flow, the resultant pressure difference was compared to the stress applied. For a 0.4ml hydrogel volume, this pressure difference was 2.72Pa (Appendix C), representing approximately 1.79% of the smallest compressive stress applied, -152Pa, corresponding to 4% strain (Appendix R). Therefore, the flow's effect on the hydrogel's strain is negligible.

For the proof of concept prototype, individual parts were manufactured and tested. Successful results suggest that a fully-functional device can be created at a later stage.

Figure 18 illustrates that the compression system produces displacements within 1.2% of the intended values. However, these measurements relate to the compression construct when disconnected from the other components. Thus, further testing is needed to verify that the complete system operates as expected. To ensure that this level of precision is maintained over a large timescale, additional reliability testing needs to be performed.

The inherent limitation of this design is the use of strain cylinders of different heights all connected to the same actuator. Hence, the duration for which the strain is applied during each cycle varies for each strain level, which does not meet the requirement of identical conditions for parallel experiments. This occurs because the 12% strain cylinder comes in contact with the hydrogel first as shown in Figure 26.

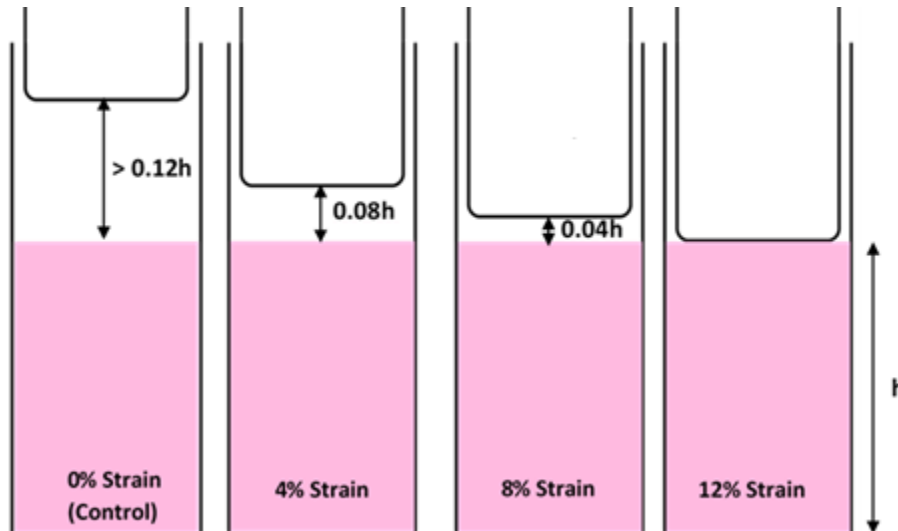


Figure 26. Strain cylinder initial positions

The strain experienced by each group of hydrogels under the assumption of compression with constant velocity is shown in Figure 27.

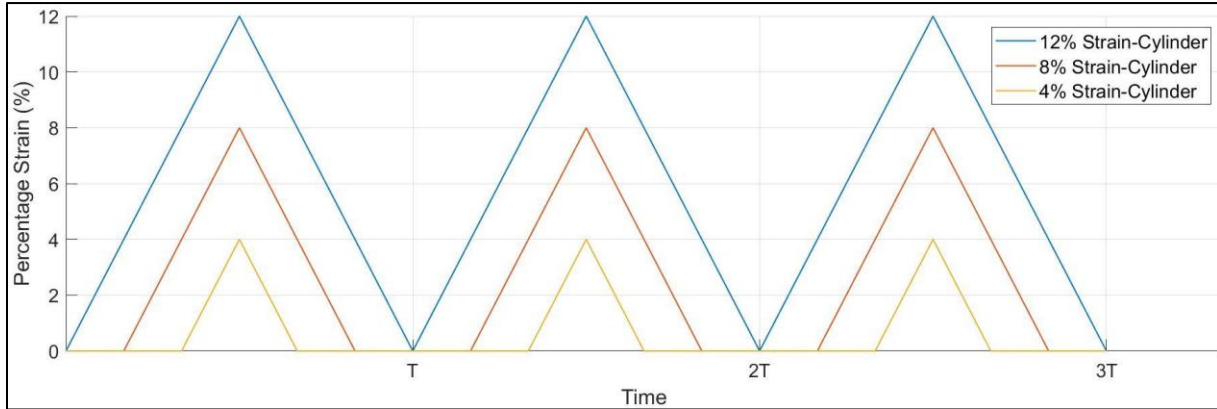


Figure 27. Hydrogel strain implemented as a triangular wave (constant actuator speed)

To mitigate this limitation, the strain must be implemented as a square wave by maximising the velocity of the actuator between the zero and maximum strain points, and then holding displacement for a set time. This requires the actuator's velocity to be large enough to produce a rise time significantly smaller than half the compression period. Simulated strain under these conditions is shown in Figure 28.

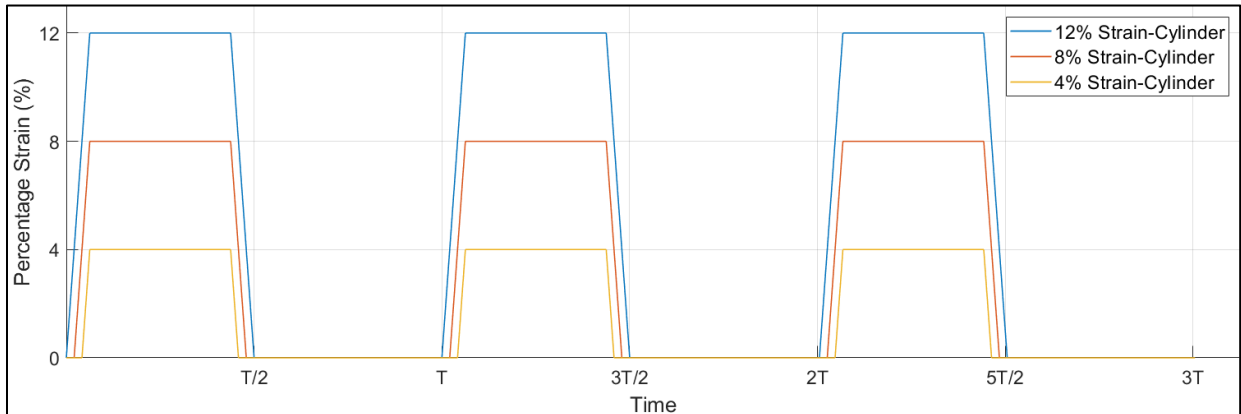


Figure 28. Hydrogel strain implemented as a square wave

An important consideration is the avoidance of air in the system. Air bubbles could cause interfacial tension to arise, resulting in cell death[25]. Furthermore, their presence could lead to flow instability. This was mitigated by the setup described in Section 2.2.

Since the device contains fluids and electronic components, safety was an important factor in the design. To minimise risk of injury, all cables will be protected by water-resistant covers. The actuator and microcontroller will be placed on top of the upper aluminium plate at a safe distance from the surface of the media-filled bottom 4-well plates.

An additional limitation of the proof of concept prototype is that medically graded O-ring silicone seals and adhesives were not used due to financial constraints. For future iterations, these must be acquired, as they come in contact with the media perfusing the cells and should be biocompatible. Proposed seals are Platinum-cured silicone gaskets[26] used in medical applications[27]. The proposed adhesive, Vitralit 7041[28], can adhere to all materials involved: ABS, glass (for the fritted discs) and

polycarbonate (for the membrane). Furthermore, ABS is not autoclavable and hence, it will be sterilised with ethylene oxide, gamma irradiation or electron beam methods[29].

Additionally, future iterations could include an actuator-compatible reflective encoder to automatically calibrate it with respect to a fixed initial position. This would improve the accuracy of the device compared to manual calibration.

The decision was made to differentiate the cells (protocol in Appendix W) after seeding in the bioreactor instead of before, as it was shown that seeding already-differentiated adipocytes causes them to rise up and become unevenly distributed throughout the hydrogel. Experimental proof of adequate perfusion will be obtained by analysing cell viability post-perfusion. Due to insufficient number of cells cultured, the remaining seeding and differentiation processes were not initiated. Therefore, a more readily available mesenchymal cell line will be cultured instead, ideally NIH/3T3 fibroblasts, owing to financial constraints.

Before and after the seeded hydrogels undergo compression, the lipid accumulation inside the adipocytes will be measured by flow cytometry, as opposed to the qualitative method of Oil Red O staining[30]. Whilst the adipocytes are undergoing their cyclic compression, their progress will be monitored by measuring the lactate dehydrogenase (LDH) and glycerol that is output into the waste reservoir. As LDH is an intracellular enzyme, its extracellular presence indicates cell death[31]. It is shown that small mechanical forces do not trigger apoptosis[32], hence no change in LDH levels is expected. The trypan blue method was initially favoured to measure this, as LDH will denature and be diluted once it is extracellular and in the reservoir, and thus will be harder to detect by assay. However, trypan blue requires hydrolysing the collagen and destroying the hydrogel[33], which would not allow real-time result monitoring afterwards. Since lipolysis produces glycerol, raised extracellular levels of glycerol indicate raised triglyceride catabolism, therefore extracellular glycerol levels inversely correlate with intracellular lipid accumulation[34].

The results have been predicted to show that cyclic compression will correlate with decreased lipid accumulation. This reflects existing literature, which indicates that compressive forces acting on the ECM of adipocytes are transmitted intracellularly via integrins[35], which regulate adhesion between cells and the ECM. These integrins transmit extracellular mechanical forces to the intracellular actin cytoskeleton. The changes in the micropillar molecular structure of the cytoskeleton trigger the MAPK/ERK pathway[36]. This is central to adipocyte differentiation, proliferation and adhesion[37] and will subsequently trigger other signalling pathways depending on the stimulus. In response to a static compressive force, the MAPK/ERK pathway downregulates PPAR γ 2 synthesis, a transcription factor that activates genes stimulating lipid uptake and adipogenesis[38]. Cyclic compression is expected to similarly activate the MAPK/ERK pathway, causing lipid accumulation to decrease.

The advantages of this experiment lie in the use of 3D cell culture, which better replicates the *in vivo* conditions compared to 2D, as the adipocytes are able to grow freely, establishing a more physiologically realistic range of transmembrane proteins[39]. Z-axis flattening from 2D cultures would otherwise affect the distribution and number of cellular junctions, such as the integrins and cadherin-catenin complexes. These, via adipokines[40], affect the actin cytoskeleton and the ECM, both essential to mechanotransduction.

Adipose tissue consists of not only mature adipocytes, but also pre-adipocytes [41]; a culture containing a range of cell maturities would better reflect the dynamic microenvironment. The enzymes and glycoproteins in adipose ECM have profound effects on adipocyte development and

metabolism[42]; implementing these proteins in the hydrogel environment would enable a more realistic adipocyte response.

Finally, hybridisation assays can additionally be performed, analysing the synthesis of key protein regulators, such as PPAR γ 2, to give a better mechanistic understanding of the underlying pathways. However, this requires the adipocytes to be destroyed, and hence the hydrogels to be permanently removed from their wells; this limitation can be overcome in a future iteration of the bioreactor using independently removable wells.

5. **Conclusion**

Through computational analysis and testing, a bioreactor design, that can provide cyclic compressions within the physiological range to 3D hydrogels, has been successfully developed. This design can be applied to study the mechanobiology of various other cell lines, as it can be also used for static compression and wider frequency ranges. With regards to adipocyte mechanobiology, this device will be utilised to accurately simulate *in vivo* conditions of adipocytes and hence provide more physiologically representative results than existing 2D methods. This leads to a better understanding of the field, which could allow development of novel methods to efficiently treat obesity.

6. References

1. National Health Service. *Statistics on Obesity, Physical Activity and Diet – England*. National Health Service. 2018. Available from: <https://digital.nhs.uk/data-and-information/publications/statistical/statistics-on-obesity-physical-activity-and-diet/statistics-on-obesity-physical-activity-and-diet-england-2018>
2. Bergman R, Kim S, Catalano K et al. Why Visceral Fat is Bad: Mechanisms of the Metabolic Syndrome. *Obesity*. 2006;14 Suppl 1:16S-19S. Available from: <https://doi.org/10.1038/oby.2006.277>
3. Yuan Y, Gao, J, Ogawa R. Mechanobiology and Mechanotherapy of Adipose Tissue – Effect of Mechanical Force on Fat Tissue Engineering. *Plastic and Reconstructive Surgery Global Open*. 2015;3(12):e578. Available from: <https://www.ncbi.nlm.nih.gov/pmc/articles/PMC4727687/>
4. Tanabe Y, Koga M, Saito M, Matsunaga Y, Nakayama K. Inhibition of adipocyte differentiation by mechanical stretching through ERK-mediated downregulation of PPAR γ 2. *Journal of cell science*. 2004 Jul 15;117(16):3605-14.
5. Hossain MG, Iwata T, Mizusawa N, Shima SW, Okutsu T, Ishimoto K, Yoshimoto K. Compressive force inhibits adipogenesis through Christmas COX-2-mediated down-regulation of PPAR γ 2 and C/EBP α . *Journal of bioscience and bioengineering*. 2010 Mar 1;109(3):297-303.
6. Shoham N, Gottlieb R, Sharabani-Yosef O, et al. Static mechanical stretching accelerates lipid production in 3T3-L1 adipocytes by activating the MEK signaling pathway. *Am J Physiol Cell Physiol*. 2012;302:C429–C441
7. Caliarì S, Burdick J. A Practical Guide to Hydrogels for Cell Culture. *Nature Methods*. 2016;13(5):405-414. Available from: <https://www.ncbi.nlm.nih.gov/pmc/articles/PMC5800304/>
8. Salazar BH, Cashion AT, Dennis RG, Birla RK. Development of a cyclic strain bioreactor for mechanical enhancement and assessment of bioengineered myocardial constructs. *Cardiovascular engineering and technology*. 2015 Dec 1;6(4):533-45.
9. Jagodzinski M, Breitbart A, Wehmeier M, Hesse E, Haasper C, Krettek C, Zeichen J, Hankemeier S. Influence of perfusion and cyclic compression on proliferation and differentiation of bone marrow stromal cells in 3-dimensional culture. *Journal of biomechanics*. 2008 Jan 1;41(9):1885-91.
10. Bölgen N, Yang Y, Korkusuz P, Güzel E, El Haj AJ, Pişkin E. Three-dimensional ingrowth of bone cells within biodegradable cryogel scaffolds in bioreactors at different regimes. *Tissue Engineering Part A*. 2008 Oct 1;14(10):1743-50.
11. Freyria AM, Yang Y, Chajra H, Rousseau CF, Ronziere MC, Herbage D, Haj AE. Optimization of dynamic culture conditions: effects on biosynthetic activities of chondrocytes grown in collagen sponges. *Tissue engineering*. 2005 May 1;11(5-6):674-84.
12. Zhang ZY, Teoh SH, Chong WS, Foo TT, Chng YC, Choolani M, Chan J. A biaxial rotating bioreactor for the culture of fetal mesenchymal stem cells for bone tissue engineering. *Biomaterials*. 2009 May 1;30(14):2694-704.
13. Subramanian G, Elsaadany M, Bialorucki C, Yildirim-Ayan E. Creating homogenous strain distribution within 3D cell-encapsulated constructs using a simple and cost-effective uniaxial tensile bioreactor: Design and validation study. *Biotechnology and bioengineering*. 2017 Aug;114(8):1878-87

14. SPI Supplies. Polycarbonate Membrane Filters: SPI-Pore Standard Polycarbonate Track Etch Membranes. Available from: <https://www.2spi.com/item/e0053-mb/polycarbonate-track-etch-membranes-13mm/> [Accessed 15th March 2019]
15. Rebet, A., MSc Research Project Report: The biophysics of resistance generation by extracellular matrix: Studies in vitro, September 2010
16. Chemglass Life Sciences. Fritted Filter Discs. Available from: <https://chemglass.com/fritted-filter-discs-1> [Accessed 15th March 2019]
17. Techsil. Panacol Vitralit 7041 UV Thixo Adhesive 100gm. Available from: <https://www.techsil.co.uk/panacol-vitralit-7041-100gm> [Accessed 15th March 2019]
18. Castro AP, Laity P, Shariatzadeh M, Wittkowske C, Holland C, Lacroix D. Combined numerical and experimental biomechanical characterization of soft collagen hydrogel substrate. *Journal of Materials Science: Materials in Medicine*. 2016 Apr 1;27(4):79.
19. Department of FEBio. FEBio Software Suite. Available from: <https://febio.org/> [Accessed 15th March 2019]
20. Grodzinsky A. *Field, Forces and Flows in Biological Systems*. Garland Science; 2011 Mar 8.
21. Qin Y, editor. *Medical textile materials*. Woodhead Publishing; 2015 Nov 21. Chapter 7, Pages 89-107.
22. Castro AP, Laity P, Shariatzadeh M, Wittkowske C, Holland C, Lacroix D. Combined numerical and experimental biomechanical characterization of soft collagen hydrogel substrate. *Journal of Materials Science: Materials in Medicine*. 2016 Apr 1;27(4):79.
23. Busby GA, Grant MH, Mackay SP, Riches PE. Confined compression of collagen hydrogels. *J Biomech*. 2013;46:837–840. doi: 10.1016/j.jbiomech.2012.11.048.
24. Ateshian GA, Warden WH, Kim JJ, Grelsamer RP, Mow VC. Finite deformation biphasic material properties of bovine articular cartilage from confined compression experiments. *Journal of biomechanics*. 1997 Nov 1;30(11-12):1157-64.
25. Elveflow. Air Bubbles and Microfluidics. Available from: <https://www.elveflow.com/microfluidic-tutorials/microfluidic-reviews-and-tutorials/air-bubbles-and-microfluidics/> [Accessed 15th March 2019]
26. TBL Plastics. High Purity Gaskets. Available from: <https://www.tblplastics.com/gaskets-high-purity/> [Accessed 15th March 2019]
27. MachineDesign. Sealing Challenges for the Medical Industry. Available from: <https://www.machinedesign.com/archive/sealing-challenges-medical-industry> [Accessed 15th March 2019]
28. Panacol Adhesives. Medical Grade Adhesive. Available from: <https://www.pandhesive-applications/medical-grade-adhesive> [Accessed 15th March 2019]
29. Industrial Specialties Mfg. Plastics Sterilization Compatibility. Available from: <http://www.industrialpec.com/images/files/plastics-sterilization-compatibility-chart-from-is-med-specialties.pdf> [Accessed 15th March 2019]
30. Kinkel AD, Fernyhough ME, Helterline DL, Vierck JL, Oberg KS, Vance TJ, Hausman GJ, Hill RA, Dodson MV. Oil red-O stains non-adipogenic cells: a precautionary note. *Cytotechnology*. 2004 Sep 1;46(1):49-56.
31. Lobner D. Comparison of the LDH and MTT assays for quantifying cell death: validity for neuronal apoptosis?. *Journal of neuroscience methods*. 2000 Mar 15;96(2):147-52.

32. Spalding KL, Arner E, Westermark PO, Bernard S, Buchholz BA, Bergmann O, Blomqvist L, Hoffstedt J, Näslund E, Britton T, Concha H. Dynamics of fat cell turnover in humans. *Nature*. 2008 Jun;453(7196):783.
33. Yan Y, Wang X, Xiong Z, Liu H, Liu F, Lin F, Wu R, Zhang R, Lu Q. Direct construction of a three-dimensional structure with cells and hydrogel. *Journal of bioactive and compatible polymers*. 2005 May;20(3):259-69.
34. Arner P. Differences in lipolysis between human subcutaneous and omental adipose tissues. *Annals of medicine*. 1995 Jan 1;27(4):435-8.
35. Juliano RL, Haskill S. Signal transduction from the extracellular matrix. *Journal of Cell Biology*. 1993 Feb 1;120:577-.
36. Paul R, Heil P, Spatz JP, Schwarz US. Propagation of mechanical stress through the actin cytoskeleton toward focal adhesions: model and experiment. *Biophysical journal*. 2008 Feb 15;94(4):1470-82.
37. Bost F, Aouadi M, Caron L, Binétruy B. The role of MAPKs in adipocyte differentiation and obesity. *Biochimie*. 2005 Jan 1;87(1):51-6.
38. Tanabe Y, Koga M, Saito M, Matsunaga Y, Nakayama K. Inhibition of adipocyte differentiation by mechanical stretching through ERK-mediated downregulation of PPAR γ 2. *Journal of cell science*. 2004 Jul 15;117(16):3605-14.
39. Wang W, Itaka K, Ohba S, Nishiyama N, Chung UI, Yamasaki Y, Kataoka K. 3D spheroid culture system on micropatterned substrates for improved differentiation efficiency of multipotent mesenchymal stem cells. *Biomaterials*. 2009 May 1;30(14):2705-15.
40. Poussin C, Hall D, Minehira K, Galzin AM, Tarussio D, Thorens B. Different transcriptional control of metabolism and extracellular matrix in visceral and subcutaneous fat of obese and rimonabant treated mice. *PloS one*. 2008 Oct 13;3(10):e3385.
41. Zuk PA, Zhu M, Ashjian P, De Ugarte DA, Huang JI, Mizuno H, Alfonso ZC, Fraser JK, Benhaim P, Hedrick MH. Human adipose tissue is a source of multipotent stem cells. *Molecular biology of the cell*. 2002 Dec 1;13(12):4279-95.
42. Bays HE, González-Campoy JM, Bray GA, Kitabchi AE, Bergman DA, Schorr AB, Rodbard HW, Henry RR. Pathogenic potential of adipose tissue and metabolic consequences of adipocyte hypertrophy and increased visceral adiposity. Expert review of cardiovascular therapy. 2008 Mar 1;6(3):343-68.

7. Appendices

Appendix A

Darcy's hydraulic resistance is given by:

$$R = \frac{\mu L}{kA}$$

μ - Dynamic viscosity

L - Length of the material in the direction of the flow

k - Darcy's permeability

A - Area of the material perpendicular to the flow

Darcy's permeability, k , for the glass frit and membrane is proportional to the square of the pore size. Table 1 shows the resistances calculations for the glass frit, the membrane and the hydrogel (without cells).

Table 1. Resistances calculations

Component	μ (cP)	L (μm)	k/μ ($\text{m}^3\text{s}/\text{kg}$)	max $K \sim (\text{min pore size})^2$ (μm^2)	A (mm^2)	R ($\text{kg}/\text{m}^4\text{s}$)
Glass frit	0.94	2000	-	100[1]	96.77	1.94×10^8
Membrane	0.94	10	-	0.0016 [2]	96.77	6.07×10^{10}
Collagen hydrogel	-	5735	0.8×10^{-10} [3]	-	96.77	4.11×10^{11}

References:

1. Chemglass Life Sciences. Filter Information. Available from: <https://chemglass.com/Themes/ChemGlass/Content/pdf/tech/Filterinformation.pdf> [Accessed 15th March 2019]
2. SPI Supplies. Polycarbonate Membrane Filters: SPI-Pore Standard Polycarbonate Track Etch Membranes. Available from: <https://www.2spi.com/item/e0053-mb/polycarbonate-track-etch-membranes-13mm/> [Accessed 15th March 2019]
3. Castro AP, Laity P, Shariatzadeh M, Wittkowske C, Holland C, Lacroix D. Combined numerical and experimental biomechanical characterization of soft collagen hydrogel substrate. *Journal of Materials Science: Materials in Medicine*. 2016 Apr 1;27(4):79.

Appendix B

For each part of the 3D printed design, more versions have been tried until the components were showing a proper fit. This meant that the bottom-inner part was sliding into the bottom-outer part but it was tight enough such that the adhesive would prevent leakages. The groove for the seal had to fit the seal and the top part with the seal attached had to slide into the bottom-inner part without requiring too much force. The glass frits had to fit in their specific positions easily, such that the glass frit would not be damaged when pressed in, but still tight enough. The dimensions of each version are shown in the table below, where: gf means glass frit, s means seal groove, r means radius, d means diameter, i means inner and o means outer.

Version	bottom-inner				top											
	di	ri	do	ro	gf di	gf ri	gf do	gf ro	s di	s ri	s do	s ro	di	ri	do	ro
1	13.9	6.95	14.8	7.4	12.2	6.1	13.2	6.6	11.1	5.55	12	6	11.1	5.55	13.2	6.6
2	14	7	15	7.5	12.2	6.1	13.2	6.6	11.1	5.55	12	6	11.1	5.55	13.2	6.6
3	14.2	7.1	15.2	7.6	12.2	6.1	13.2	6.6	11.1	5.55	12	6	11.1	5.55	13.2	6.6
4	13.9	6.95	14.8	7.4	12.2	6.1	13.2	6.6	11.1	5.55	12	6	11.1	5.55	13.2	6.6
5	14	7	15	7.5	12.3	6.15	13.3	6.65	11.1	5.55	12	6	11.1	5.55	13.3	6.65
6	14.1	7.05	15.1	7.55	12.4	6.2	13.4	6.7	11.1	5.55	12.2	6.1	11.1	5.55	13.4	6.7
7	13.9	6.95	14.8	7.4	12.5	6.25	13.5	6.75	11.1	5.55	12.3	6.15	11.1	5.55	13.5	6.75
8	13.9	6.95	14.8	7.4	12.2	6.1	13.2	6.6	11.1	5.55	12.4	6.2	11.1	5.55	13.2	6.6
9	13	6.5	15	7.5	12.5	6.25	14	7	12	6	13	6.5	12	6	14	7
10	14	7	16	8	12.5	6.25	15	7.5	11.6	5.8	12.5	6.25	11.6	5.8	15	7.5
11	15	7.5	16	8												
12	16	8	17	8.5												
13	14.5	7.25	15.5	7.75												
14	14.6	7.3	15.6	7.8												
15	14.7	7.35	15.7	7.85												
16	14.8	7.4	15.8	7.9	16 is tighter, might need too much force to push it in											
17	14.9	7.45	15.9	7.95	17 is ok in terms of pressure but has more leakage											
18	15	7.5	16	8												

bottom_outer						
di smaller	ri smaller	di larger	ri larger	ro	do	
11.1	5.55	15.5	7.75	8.25	16.5	
11.1	5.55	15.6	7.8	8.3	16.6	
11.1	5.55	15.7	7.85	8.35	16.7	
11.1	5.55	15.8	7.9	8.4	16.8	
11.1	5.55	16	8	8.5	17	
11.1	5.55	16.2	8.1	8.6	17.2	
11.1	5.55	16.4	8.2	8.7	17.4	
11.1	5.55	16.6	8.3	8.8	17.6	fits V16 of bottom_inner
11.1	5.55	16.8	8.4	8.9	17.8	fits V17 of bottom_inner
11.1	5.55	17	8.5	9	18	

	good values
	values that would not fit gf or s
	the chosen value

Appendix C

The flow rate used by this study [1] was 4ml/h for a 3D bioreactor containing 8×10^7 adipose-derived stem cells. The volume of this bioreactor was 8ml, resulting in a flow rate of 4 ml/h required for a cell density of 10^7 cells/ml. Assuming a linear relationship, it means that for 50,000 cells/ml used in our project, a 20×10^{-3} ml/h flow is required.

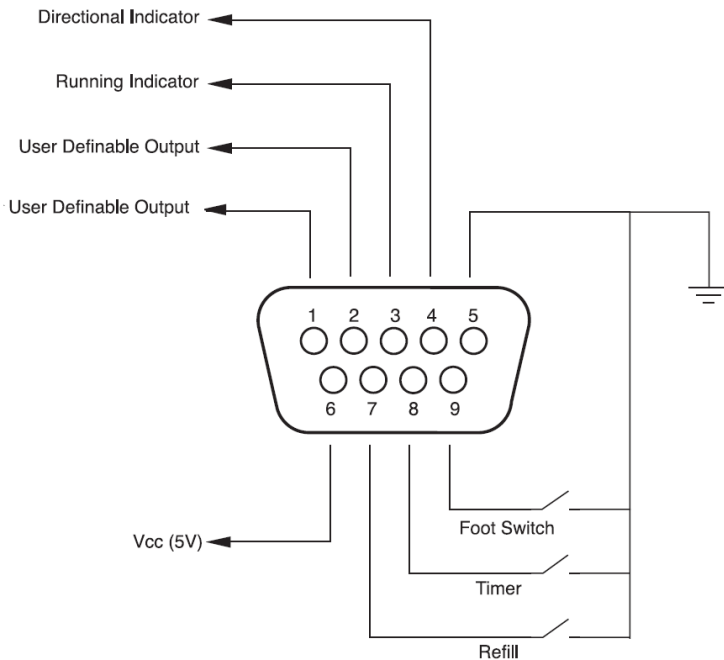
Using $\Delta P = QR$, where $R = 4.11 \times 10^{11}$ kg/m²s
(see appendix A)

$\Rightarrow \Delta P = 2.72$ Pa

Reference: [1] Gerlach JC, Lin YC, Brayfield CA, Minter DM, Li H, Rubin JP, Marra KG. Adipogenesis of human adipose-derived stem cells within three-dimensional hollow fiber-based bioreactors. Tissue Engineering Part C: Methods. 2011 Oct 13;18(1):54-61.

Appendix D

TTL serial (transistor-transistor logic) is a serial communication method. Serial communication at a TTL level means that 0-0.5V represents a digital low and 2-5V is regarded as digital high. This protocol is used by many microprocessors, including Arduino, for serial communication compared to RS-232 protocol that uses bipolar voltages to define digital zero and one. Pump 33 DDS used in this device contains a 9-pin TTL port that allows pump operations to be synchronised with external devices.



The Pin we are interested in is Pin 4 which is the pump directional indicator. Digital LOW means syringe 1 is infusing whilst digital HIGH means syringe 1 is refilling.

TTL port pinout was obtained from “Harvard Apparatus Model 33 Twin Syringe Pump User's Manual”.

Appendix E

```
int Valve1 = 13; // red LED connected to digital pin 13
int Valve2 = 12; // green LED connected to digital pin 12
int inPin = 7; // pump TTL pin 4 is connected to digital pin 7
int val = 0; // variable to store the read value

void setup() {
  pinMode(Valve1, OUTPUT); // sets the digital pin 13 as output
  pinMode(Valve2, OUTPUT); // sets the digital pin 12 as output
  pinMode(inPin, INPUT); // sets the digital pin 7 as input
  Serial.begin(9600);
}

void loop() {
  val = digitalRead(inPin); // read the input pin
  if (val == HIGH)
  {
    digitalWrite(Valve1, HIGH); // sets the red LED to high value
    digitalWrite(Valve2, LOW);
    Serial.println("Valve 1 should be on");
  }
  if (val == LOW)
  {
    digitalWrite(Valve2, HIGH);
    digitalWrite(Valve1, LOW);
    Serial.println("Valve 2 should be on");
  }
  Serial.println(val);
}
```

Appendix F

An order of magnitude calculation for the resistance of each of the 16 branches of the tubing circuitry, given that cell culture medium viscosity in the order of 10^{-3} Pa s, tube length in each branch is in order of 10^{-1} m and tubes have radius order of 10^{-3} m:

$$R_{tube} = \frac{8\mu L}{\pi r^4} \approx \frac{8 \cdot 10^{-3} \cdot 10^{-1}}{\pi \cdot 10^{-12}} = 10^9 \frac{kg}{m^4s}$$

The hydrogel resistance is in the order of 10^{11} kg m⁻⁴s⁻¹, which means that the total resistance of each branch is approximately equal to the resistance of the hydrogel. Thus, the volumetric flow rate across the kth hydrogel, with resistance R_k , can be calculated by:

$$Q_k = \frac{R_p}{R_k} Q_{pump}, \text{ where } R_p = \frac{1}{\sum_{i=1}^{16} \frac{1}{R_i}} \text{ is the total resistance of the all 16 branches in parallel.}$$

As such we can conclude that for 16 hydrogels with similar resistance values, the flow will be split evenly across all wells ($Q_k \approx \frac{Q_{pump}}{16} \forall k$).

Appendix G

A test was performed to check the approximate force needed to push the strain cylinder against the collagen-hydrogel chamber, due to the limited force per well the actuator can supply. The setup is shown in Figure 1. Weights were placed in increments of 100g until the top cylinder started to slide into the bottom one, at which point, static friction between the seal and the cylinder was overcome. This force was found to be close to the actuator's capabilities per well (7.848N), well within the capabilities. As shown in Methods, the maximum stress needed to be supplied by the actuator to compress the hydrogel is approximately 400Pa, which corresponds to a force of 0.07N which is negligible in comparison, so this test was sufficient regarding this aspect.



Figure 1. Test setup for estimating the friction force due to the seal

Appendix H

During each cycle, all hydrogels should reach their prescribed strain level and relax back to 0% strain. Thus, the displacement of the actuator is given by $2 \cdot \epsilon_{max} \cdot w$, where w is the hydrogel height and ϵ_{max} is the maximum strain applied to any of the hydrogel. For compressions at constant velocity, the speed of the actuator is related to the compression frequency by: $f \cdot 2 \cdot \epsilon_{max} \cdot w = v$.

Hence, for $\epsilon_{max}=12\%$ and $v < 5mm s^{-1}$ the maximum frequency that can be implemented is equal to:

$$f_{max} = \frac{5mm s^{-1}}{0.24 \cdot w} = \frac{20.83mm s^{-1}}{w}$$

This means that the frequency range of 0.1Hz to 1Hz can be implemented for hydrogel heights of less than 20.83mm.

Appendix I

The actuator resolution, δ , sets a bound for the error in the strain provided to the hydrogels. When aiming for a strain level ϵ , the real strain applied is given by:

$$\epsilon = \frac{\Delta w \pm \delta}{w} = \epsilon_{ideal} \pm \frac{\delta}{w}$$

Hence, absolute error of less than 0.001 (0.1% strain) the resolution must be 1000 times smaller than the hydrogel height. The actuator chosen has resolution 0.005mm, which means that the error is 0.001 for heights larger than 5mm. For heights less than 5mm micro-stepping must be used. The motor-driver used allows for micro-steps down to 1/8 of the original step size. Thus, the resolution can be improved to 0.000625mm and the error less than 0.001 for heights larger than 0.625mm

Appendix J

For microstepping mode: The displacement is equal to 0.005mm/8 per falling edge. So for a constant velocity motion that reaches a value of X millimeters after T/2 seconds, we must send $8X/0.005=1600X$ pulses spaced equally in the T/2 seconds. Hence, we set a square wave that has period T/(3200X) with a high duration of T/(6400X) and a low duration of T/(6400X).

```

unsigned long freq=10;           //in 10ths of Hz (10 corresponds to 1Hz). To
set the period to 1/f
unsigned long X=500;           //displacement in micrometers
int actuator=15;             // SMC connection
int dir=14;                 //direction of actuator
unsigned long pulse_width=10000000/(64*X*freq);
unsigned long period_ideal=5000000/freq; // T/2
unsigned long period=0;

void setup()
{
  pinMode(actuator, OUTPUT);
  pinMode(dir, OUTPUT);
}

void loop() {
  digitalWrite(dir, HIGH);
  period=0;
  while (period<period_ideal) {
    digitalWrite(actuator, HIGH);    // sets the digital pin 15
    delayMicroseconds(pulse_width); // pulse high
    digitalWrite(actuator, LOW);
    delayMicroseconds(pulse_width); // pulse low
    period=period+2*pulse_width;
  }
  digitalWrite(dir, LOW);
  period=0;
  while (period<period_ideal) {
    digitalWrite(actuator, HIGH);    // sets the digital pin 15
    delayMicroseconds(pulse_width); // pulse high
    digitalWrite(actuator, LOW);
    delayMicroseconds(pulse_width); // pulse low
    period=period+2*pulse_width;
  }
}

```

Appendix K

Protocol for Cell Culture and Passage

Create a medium of DMEM high glucose, 10% of FBS and 1% of PenStrep;

Thaw cells:

- (2) Fill a 10 ml tube with 9ml of cell culture medium and let it warm up in the water bath;
- (1) Take out the cryotube from the nitrogen liquid tank;
- (3) With a tweezers keep the cryotube on the water bath at 37°C until be liquid. Note: other way to do it is: place small quantities of media inside of the cryotube following place in the 10ml tube - do it a couple of times;
- (4) Centrifuge during 5 min at 200g;
- (4) Remove supernatant;
- (5) Re-suspend the pellet in 1ml of media, make sure you do it very gently, without creating bubbles;
- (6) Re-suspend the cell suspension in the desired volume of media and transfer to a T-flask or Petri Dish;
- (7) Leave at 37°C supplied with CO₂.

Cell Passage:

- (1) Take out all media from the flask;
- (2) Add 5ml of PBS1x to rise the cells; Agitate it slowly. Remove the PBS after 1-5 min. Repeat once again (not mandatory this last step);
- (3) Add 1ml (volume depends on the surface) of trypsin on the top of the cell monolayer. Leave for 2 minutes in the incubator;
- (4) Look on the microscope if the cells are already detached;
- (5) Add 9 ml of medium to the plate in order to inactivate the effect of the trypsin and collect all the solution to a 10 ml tube;
- (6) Centrifuge the tube during 5 min at 1200 rpm;
- (7) Re-suspend the pellet in 1ml of media, please make sure you are gentle without creating any bubbles;
- (8) Re-suspend the cell suspension in the desired volume of media and transfer to a T-flask or Petri Dish.

Cell Preservation:

- (1) Perform a cell suspension solution (it could be either in cell culture medium or in FBS inactivated).
- (2) Perform a cell counting in order to know the cell concentration.
- (3) Use a cryotube of 1ml and label it;
- (4) Make 1 ml of DMEM 10%FBS,1%PS and 5% of DMSO (Dimethyl Sulphoxide for cell culture);
- (5) Place the cryotube in a cryobox and store at -80°C overnight.
- (6) Transfer to -120°C.

Appendix L

Cell Viability Testing with Trypan Blue Exclusion Method

The Trypan Blue dye exclusion test is used to determine the number of viable cells present in a cell suspension. It is based on the principle that live cells possess intact cell membranes that exclude certain dyes, such as trypan blue, Eosin, or propidium, whereas dead cells do not. When a cell suspension is simply mixed with the dye and then visually examined to determine whether cells take up or exclude dye. A viable cell will have a clear cytoplasm whereas a nonviable cell will have a blue cytoplasm.

Periodic cell viability assessment provides an early indicator of the quality of your fresh cells prior to freezing. Viabilities of greater than or equal to 95% are excellent.

Safety Precautions

Use personal protective equipment when performing this assay, such as gloves and a lab coat. According to the Material Safety Data Sheet (MSDS), trypan blue may cause cancer, so practice appropriate laboratory safety methods.

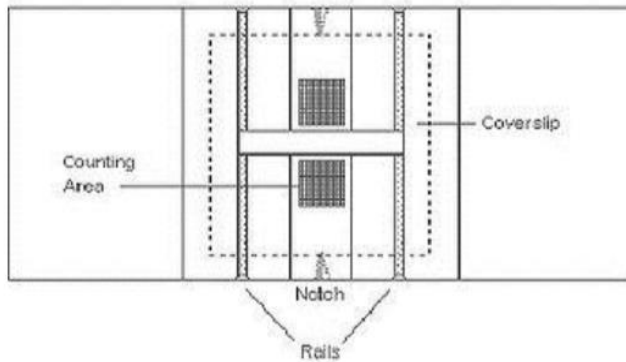
Equipment and Supplies

Pipette and tips
Trypan Blue
Hemocytometer and coverslip
Cryovials
Microscope
Counter

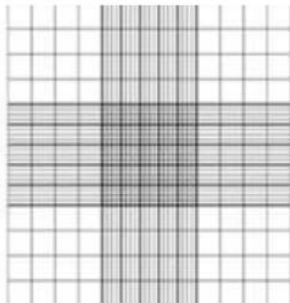
Procedure

- (1) Place 50 μ l of cell suspension in a cryo-vial.
 - (2) Add equal parts of 0.4% trypan blue dye to the cell suspension to obtain a 1 to 2 dilution (example: 50 μ l of cells to 50 μ l of trypan blue) and mix by pipetting up and down.
 - (3) Incubate mixture for less than three minutes at room temperature. If cells are counted after approximately five minutes, viability will be inaccurate due to cell death.
-

- (4) With the cover slip already in place, fill one side of a hemacytometer counter with the cell suspension by placing the tip of the pipette at the notch. Typically, each side will take 10 to 20 μl .



- (5) Place the hemacytometer on the stage of a light microscope and focus onto the cells.
- (6) Each side of the hemacytometer contains multiple squares. Count all cells (clear and blue) in each large square in each corner of the hemacytometer (see the white areas in the diagram below). Each large square contains 16 small squares. In each large square count cells that are on the border lines on two sides only. Keep track of the number of blue cells separately as well as part of the complete number of cells. Blue cells are the non-viable cells.



- (7) Calculate the percentage of viable cells by dividing the number of viable cells by the number of total cells and multiplying by 100 or $\% \text{ viable cells} = [1.00 - (\text{Number of blue cells} \div \text{Number of total cells})] \times 100$.
- (8) Alert your supervisor or lab director if the viability is less than 90%. Document your results on the W drive.

Appendix M

Protocol for extracting collagen

Equipment:

- Scalpel (#4)
- Hemostat
- Acetic acid
- UltraCentrifuge
- Microdissecting forceps (1x2 teeth), 2 pairs
- Frozen rat tails (3 – 4 for around 1 gram of tail tendons)
- 70% (v/v) ethanol
- 50 ml conical centrifuge tubes)
- Large Petri dish
- 250 ml glass bottle
- 400 ml glass bottle
- Nalgene vacuum filter unit, 150 ml

Technique:

Part 1: Extracting the Tendons

1. Autoclave 250 and 400 ml glass bottles as well as, scalpel, hemostat, and forceps to ensure sterility. The protocol will be performed under ethanol. Fill the 250 ml bottle with 70% ethanol and add it and the petri dish to the hood. Pour ethanol into the Petri dish near to filling. Refill the 250 ml bottle with 70% ethanol.
2. Add rat tails to the petri dish with ethanol. Let the rat tails thaw for 10 – 20 minutes. Cut off the very tips of the tail at both ends. Using the hemostat, hold the tail under ethanol and make an incision along the tail from one end to the other. Make sure the incision is fairly shallow so that you are only cutting the skin. Then peel the skin away using the hemostat and forceps (as though you were peeling a banana).
3. Now, the tendon bundles are now visible as long silvery white fibers extending down the length of the tail. Holding the tail at the end (use either forceps or hemostat, whatever is more comfortable), grab a few tendons at the tip with the microdissecting forceps, and pull the tendons out of their sheaths in the direction of the tail end (do not pull towards the base of the tail as they are more likely to fracture). Place the tendons in the 250 ml bottle of ethanol. Continue moving down the tails and pulling tendons until the rate of fracture becomes high.
4. Once extraction is complete, pat dry the tendons with Kim wipes, and weigh them. In order to maintain sterility, weigh the collagen in the 50 ml conical tubes. Using the acetic acid, create a 0.1% Acetic Acid solution. Place the tendons in the 400 ml bottle, and add 0.1% acetic acid solution at 150 ml/gram of tendon. Allow collagen to solubilise for at least 48 hours at 4°C. During this time, the tendons will swell to occupy a large part of the total volume.

Appendix N

Part 2: Spinning down and reconstituting the collagen

1. Place the collagen solution equally into 50 ml conical centrifuge tubes, making sure the tubes are at least two thirds full. Weigh the tubes carefully, making sure that the tubes to be directly opposite from each other are perfectly balanced (± 0.1 gram). If using the NBTC Centrifuge, set centrifuge to highest settings (9000 rpm, fast ramp up, fast ramp down) for 90 minutes to remove unsolubilised collagen, blood, muscle tissue, etc... from solubilised collagen.
2. Collect the clear supernatant and discard the pellet. If the pellet is disturbed during collection, spin down the collagen again at the above settings. Place supernatant in collection flask of a Nalgene vacuum filter unit, screw the filter back on, and freeze the solution in -80°C for 30 minutes. Place the entire unit on a lyophilizer for 48 hours. Using a vacuum filter unit in this manner will further ensure the sterility of the collagen product.
3. Weigh the collagen product and reconstitute in 0.1% acetic acid at the desired concentration. If the collagen will not be used immediately, reconstitute it at a dilute concentration (i.e. 6 mg/ml) and store at 4°C .

Appendix O

100 μl of NaOH 0.34N were mixed with 100 μl of MEM10x and 25 μl of HEPES. To this, 800 μl of the collagen stock solution was added. The sample should have a pink colour due to the phenol red in the MEM10x solution (Figure 1), which indicates a basic environment. The collagen will start polymerising, process which can be catalysed by incubating at 37°C for 25 minutes.

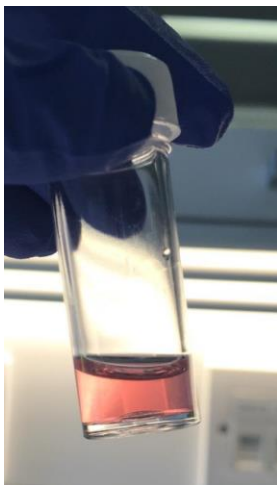
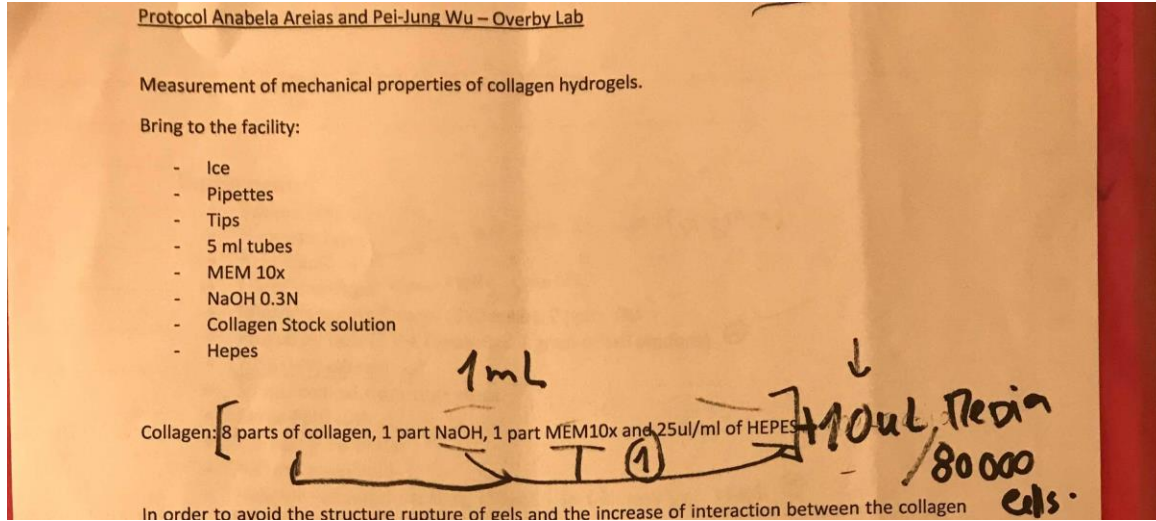


Figure 1. Pink hydrogel

The original protocol paper, given by Anabela Cepa-Areias is shown below:



Appendix P

Table 1. Rheometry experiment setup

1: Conditioning Sample Name: Conditioning Step Enabled: yes Temperature: 25 °C Inherit Set Point: No Wait for temperature: Yes Wait for axial force: No Perform preshear: No Perform equilibration: Yes Equilibration time: 30.0 s	2: Oscillation Amplitude Name: Strain sweep step Enabled: yes Temperature: 25 °C Soak time: 60.0 s Wait for temperature: No Frequency: 0.1 Hz Amplitude ramp type: Log Strain %: 0.05 % End strain %: 5.0 % Points per decade: 5 Controlled strain type: Continuous oscillation [direct strain] Motor mode: Auto Conditioning time: 3.0 s Sample time: 3.0 s Termination comparison enabled: No Termination equilibrium enabled: No	3: Oscillation Frequency Name: Frequency sweep step Enabled: yes Temperature: 25 °C Soak time: 60.0 s Wait for temperature: No Strain %: 1.0 % Frequency ramp type: Log Frequency: 0.1 Hz End frequency: 5.0 Hz Frequency points per decade: 5 Controlled strain type: Continuous oscillation [direct strain] Motor mode: Auto Conditioning time: 3.0 s Sample time: 3.0 s Termination comparison enabled: No Termination equilibrium enabled: No
4: Conditioning End Of Test Name: Post-Experiment Step Enabled: yes Set temperature: No Set temperature system idle: No		

Table 2. Rheometry summarised data

	1mg/ml		2mg/ml		4mg/ml		8mg/ml	
1	9.13618	8.07416	69.0383	16.6964	217.126	36.8114	402.438	50
2	9.47852	0.59186	56.9201	3.55507	205.972	38.1958	554.121	54.437
3	10.2131	1.04331	53.6774	6.56904	205.812	35.2353	565.152	45.6742
4	10.2754	0.93091	52.5874	5.85878	203.177	31.7478	538.994	53.8204
5	10.2903	0.95550	53.3363	5.49587	195.778	30.704	548.386	53.5616
6	10.2535	0.89595	53.5135	5.64988	186.212	29.2344	556.011	53.1977
7	10.1304	0.91269	54.4821	4.88102	174.333	27.2486	561.609	49.4568
8	9.97156	0.92198	55.6623	4.48219	162.83	25.0501	568.645	49.3443
9	9.83669	0.88988	55.4025	5.7288	152.572	21.2661	569.731	52.874
10	9.7451	0.88918	54.9147	4.68551	204.246	67.2296	572.765	46.9325

11	9.76879	0.83032	57.3015	5.27208	44.2561	N/A	592.68	46.108
Average	9.91814	1.53961	56.0760	6.26133	190.805	34.2723	548.230	50.5406
Std Dev	0.37109	2.17010	4.54692	3.55312	48.5465	12.7234	50.3568	3.44035
E*	29.6089368		166.4522452		571.8850594		1624.136933	
G*	10.03692773		56.4244899		193.8593422		550.5548924	

Appendix Q

clear all

$u0 = 5.735 \cdot (10^{-4});$

$L = 5.735 \cdot (10^{-3});$

$H = 4035.403;$

$k = 0.8 \cdot (10^{-10});$

figure

time = 1;

for t=0:5:40

space = 1;

for x1 = 0:0.0001:0.005735

sum = 0;

for n = 1:10000

sum = sum + $((2 \cdot u0) / (n \cdot \pi)) \cdot \sin((n \cdot \pi \cdot x1) / L) \cdot \exp(-t / ((L^2) / ((n^2) \cdot (\pi^2) \cdot H \cdot k)));$

end

u1(space,time) = $u0 \cdot (1 - x1 / L) - \text{sum};$

space = space + 1;

end

x = 0:0.0001:0.005735;

plot(x,u1(:,time));

hold on

time = time + 1;

end

xlabel('x1 (m)');

ylabel('u1 (m)');

title('Displacement profiles');

Appendix R

The method used is to prescribe the hydrogel the strain in question and then observe the compressive stress present within the structure. The result is shown for 12% strain in Figure 1.

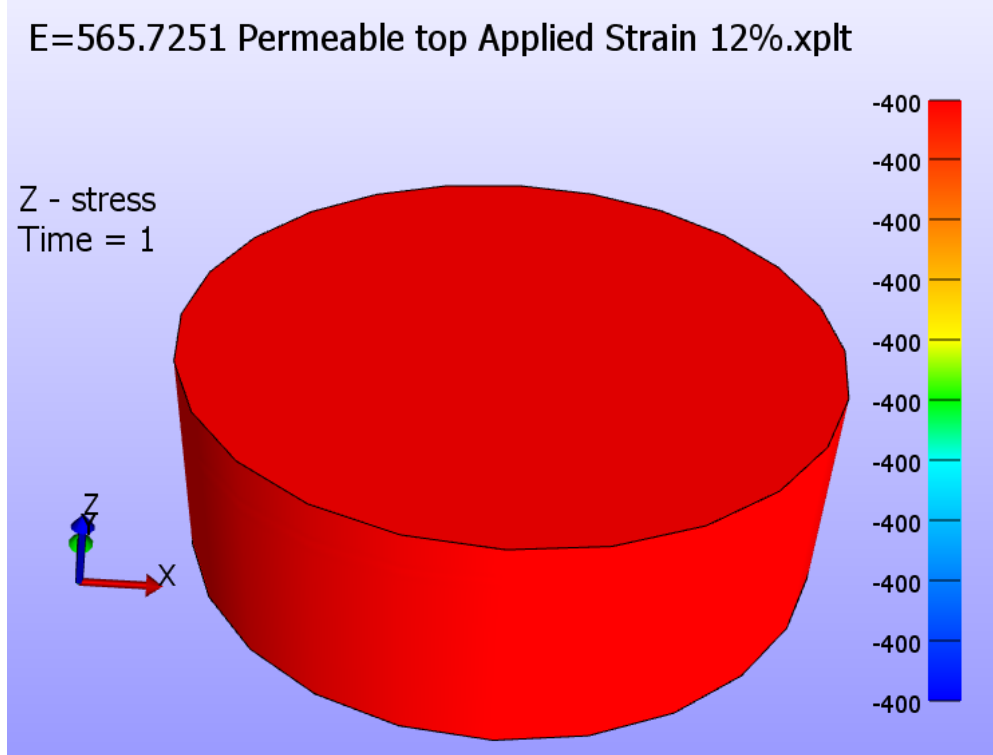


Figure 1. Stress resulting from applying a 12% strain to the hydrogel model.

The method was repeated for the other strains: 4% and 8%. The 10% strain was also simulated for the book proof. Then, to compress the model to the desired strain, the stress obtained in these simulations was applied. Table 1 shows the resulting stresses for each strain level.

Table 1. Resulting compressive stresses for each strain level.

Strain level (%)	Stress (Pa)
4	-152
8	-285
12	-400
10	-344

Appendix S

The mesh corresponding to the hydrogel model is shown below:

Porous top	<ul style="list-style-type: none"> • Wedge-centre mesh • 4 slices, 1 segment, 24 stacks • 425 nodes • Z-bias: 0.9 – finer mesh on the upper boundary
Porous top and bottom	<ul style="list-style-type: none"> • Wedge-centre mesh • 4 slices, 1 segment, 120 stacks • 2057 nodes • Mirrored Z-bias: 1.2 – finer mesh on the upper and bottom boundaries.

Appendix T

Frequency (Hz)	Time (s)	Number of Falling Edges	Theoretical		Experimental			
			Displacement (µm)	Strain (%)	Displacement (µm)	Strain (%)	Displacement per edge (µm)	Full step (µm)
10	32	320	200	3.49	220	3.84	0.689	5.5
20	24	480	300	5.23	260	4.53	0.542	4.333
20	32	640	400	6.97	400	6.97	0.625	5
40	20	800	500	8.72	520	9.07	0.65	5.2
40	24	960	600	10.46	640	11.16	0.667	5.333
40	28	1120	700	12.21	680	11.86	0.607	4.857
40	32	1280	800	13.95	820	14.30	0.641	5.125
60	24	1440	900	15.69	940	16.39	0.653	5.222
80	20	1600	1000	17.44	1040	18.13	0.65	5.2

Appendix U

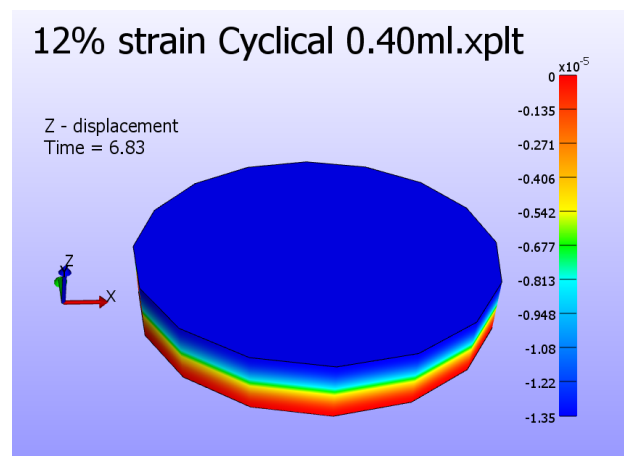
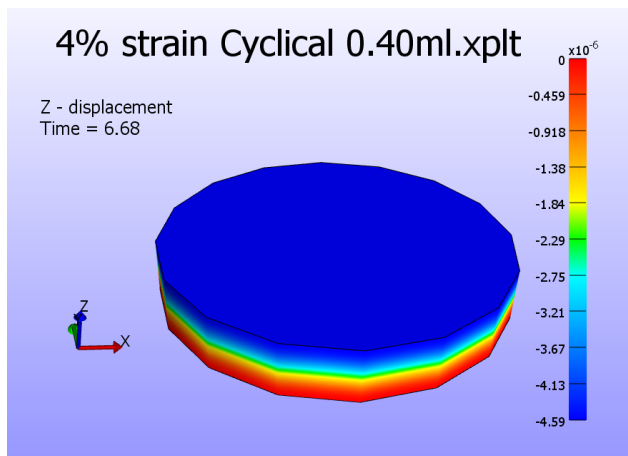
Strain was constant at 8% for all the values in the table below.

Volume (ml)	Height (m)	Time to relaxation (s)
1	0.005735	30.20
0.9	0.0051615	24.13
0.8	0.004588	19.73
0.7	0.0040145	14.62
0.6	0.003441	10.8

0.55	0.00315425	8.96
0.5	0.0028675	7.4
0.45	0.00258075	6.033
0.4	0.002294	4.75
0.35	0.00200725	3.64
0.3	0.0017205	2.68
0.25	0.00143375	1.86
0.2	0.001147	1.2
0.15	0.00086025	0.68
0.1	0.0005735	0.31
0.05	0.00028675	0.09

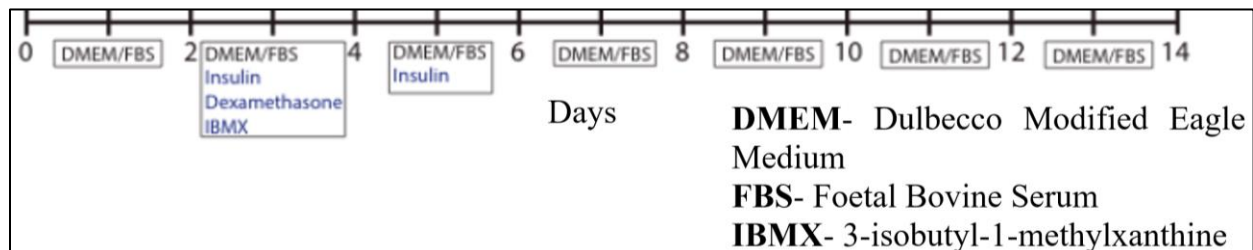
Appendix V

The relaxation time for 4% strain is 4.68 s, shown below. The relaxation time for 12% strain is 4.83s, shown below as well.



Appendix W

Differentiation Protocol



Contribution Statements

Beatrice-Cristina Bezdadea

- CAD
- FEBio
- Rheometry
- Hydrogel preparation from collagen solutions
- Final report writing and editing

Rares-Andrei Dorcioman

- FEBio
- CAD
- Rheometry
- Final report writing and editing

Charalambos Hadjipanayi

- Design of Compression system
- Manufacturing compression system
- Design of perfusion system
- Programming of Central Microcontroller
- Final report writing and editing

Emmanuel Gkigkilinis

- Final report writing and editing
- FEBio
- Rheometry

Georgios Gryparis

- Design of Compression system
- Manufacturing compression system
- Design of perfusion system
- Programming of Central Microcontroller
- Final report writing and editing

Akanksha Gupta

- Collagen constitution
- 3T3-L1 thawing
- 3T3-L1 cell culture
- Final report writing and editing
- Cell Culture Training

Goutham Sathyanarayanan

- Collagen extraction
- Collagen lyophilising
- 3T3-L1 cell culture
- Final report writing and editing
- Flow Cytometry training
- Cell Culture Training

Andrew Ting

- Collagen extraction
- 3T3-L1 thawing
- 3T3-L1 cell culture
- Final report writing and editing
- Flow Cytometry training
- Cell Culture Training